INVESTIGATION OF THE ANCHORAGE BEHAVIOR OF HEADED REINFORCING BARS USING THE FINITE ELEMENT METHOD

By
Jianjun Wu and
Steven L. McCabe

Structural Engineering and Engineering Materials
SM Report No. 49

UNIVERSITY OF KANSAS CENTER FOR RESEARCH, INC.
LAWRENCE, KANSAS
April 1998

ACKNOWLEDGEMENTS

This study was supported in part by the KU Transportation Center and by the Department of Civil and Environmental Engineering at the University of Kansas. The authors gratefully acknowledge this support.

Table of Contents

CHAPTER 1

Introduction

1.1 Headed Reinforcing Bar

A headed reinforcing bar is a new type of reinforcement with a T-shaped anchor connected to the end of a reinforcing bar. Conceptually, the bar is usually a tension member or compression one depending on structural engineering applications. The T-shaped anchor, referred to as head in the rest of this report is a relatively stiff steel "plate " in terms of its structural behavior. When embedded in concrete, the head provides anchorage for the bar to which it is attached, so that the tension or compression force can be developed in the bar. Practically, in reinforced concrete structures, the reinforcing bar can be simply a deformed bar or a round steel bar. The head could be a small piece of steel "plate" in any realistic shape providing that it functions as an anchor, meets economical considerations, and fits the individual application. The head investigated in this project is a square plate shown in Fig. 1.1-1 below.

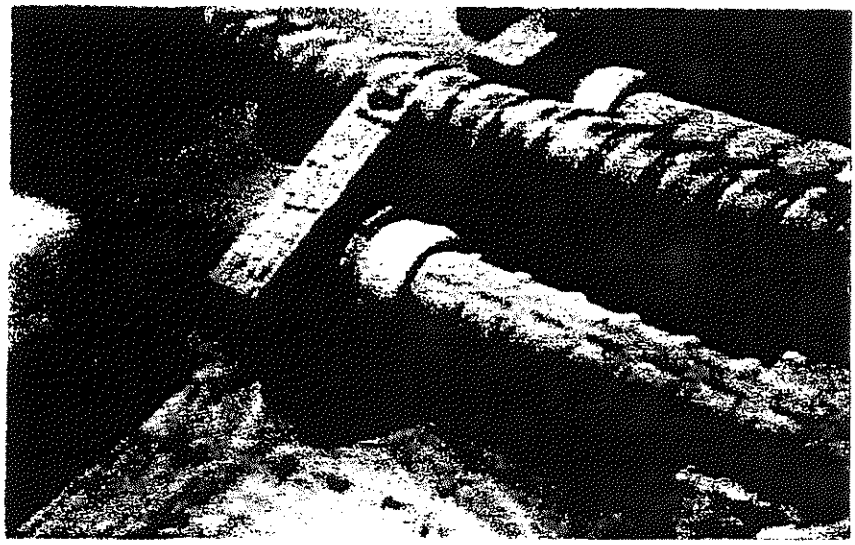

Fig. 1.1-1

The connection between the head and the bar should be strong enough so that the yield force in the bar can be developed. Therefore, the head should be forged or welded to the end of the bar. One such welding process is friction-welding whereby the friction between a bar and plate when moved relative to one another meets two together. As an alternative, the head might be screwed to the end of a bar like the relationship between a nut and the threaded end of a bolt.

1.2 Advantage of Headed Reinforcing Bars

There are some reasons for engineers to use headed reinforcing bars instead of conventional bars in structural design and construction. First, using a headed bar uses the advantage of the effective anchorage property of the head. It is not difficult for a structural engineer to understand that one can obtain much better anchorage for his or her reinforcement design by using a headed bar than by using a bar with anchorage along its length. Even for one who is not an engineer, for example, can tell the difference between pulling a wood pile embedded in soil and dragging a tree trunk with roots underneath out of ground. Obviously, the same concept applies in the anchorage behavior of a traditional bar and a headed bar.

Second, using a headed bar is simpler than using traditional deformed bar in terms of material and anchorage. The basic principle of a reinforced concrete structure is that the bar and concrete can work together as a structure in which the concrete is under compression only and the bar is subjected to tension. The compatibility of these two different materials is based on the bond strength between the interface of steel bar and concrete. Determining the bond strength is complicated because there are many related factors involved such as concrete strength, friction between the steel and concrete, roughness of bar surface, confinement and more. However, the interlock action between the rib of a deformed bar and concrete is a major factor to bond strength. Approximately,

the interlock is proportional to the localized concrete bearing strength under the equivalent surface projected from the rib of a deformed bar. From this point of view, the bigger the projected surface, the higher the bearing strength. For practical reasons, it is not reasonable or economical to project all ribs out too far along the bar. Moreover, higher bearing on the ribs will result in higher splitting stresses as well. Placing a small head at one or both ends of a bar offers a better solution to the problem since anchorage can be provided in a simple efficient manner.

The real advantage of using a headed bar is not only a better method of improving bar anchorage behavior, but a practical solution to construction problems. Anyone who has visited a construction site has seen "reinforcement congestion" at many joints in reinforced concrete structures , especially construction in seismic regions. This congestion occurs because of the bars coming into these joints. To mention just one example, at a typical interior beam to column joint in a reinforced concrete frame, there are bars in the column go through the joint from the lower level story to the upper story plus column ties; and at least four beams come to the column from the all directions with many reinforcing bars crossing over the joint. Also, the bars from the beams cannot be cut off at the column faces but beyond a distance and bent, or using a standard 90 degree or 180 degree hooks in some cases, so that the bars can meet development requirements. Consequently, from the view of construction practice, this type of "reinforcement congestion" causes a difficult situation for construction workers to set reinforcement and place concrete during construction. From a structural engineer's view, the congestion also reduces the structural ductility due to localized "over-reinforced" regions around the joint. If a headed bar can be employed and a portion of the bar development length is eliminated, it becomes helpful option that can be used to improve the reinforcement congestion situation in these joints.

Because of the advantages of headed bars, they already have been used in civil engineering projects around the world. For example, the Hibernia Project, located off the coast of St. John's Newfoundland, is an approximate by 5 billion dollar undertaking by several countries to construct an off-shore oil platform. The structure requires about

70,000 tons of steel reinforcement. This creates congestion problems and made the headed bars the only means of achieving some of the structural design requirements. Standard hooks and bent stirrups were impractical (Wright and McCabe, 1997).

1.3 Purpose of Investigation

Although headed reinforcing bars have been used in reinforced concrete structures for several years, there are no specific design provisions for headed bar design and construction in related American building codes, such as the ACI building code. Some research on headed reinforcing bar anchorage behavior has been conducted in the United States and Canada in order to provide more data and reference information for adoption of building code such as ACI. One of these projects, has been completed by Wright and McCabe at the University of Kansas (1997). In this research, the anchorage behavior of headed bars embedded in concrete was investigated by using several groups of concrete beam end specimens. A total of 72 tests were run. A typical experimental specimen is a concrete block of 9" X 18" X 24" (about 230 mm X 460 mm X 610 mm) with a headed bar embedded in it. For operational considerations, the headed bar is poured with the bar in the bottom of the specimen usually placed at top position of the concrete block like the top bars in a concrete beam. Fig. 1.3-1 shows the specimen under testing in the structural laboratory of University of Kansas.

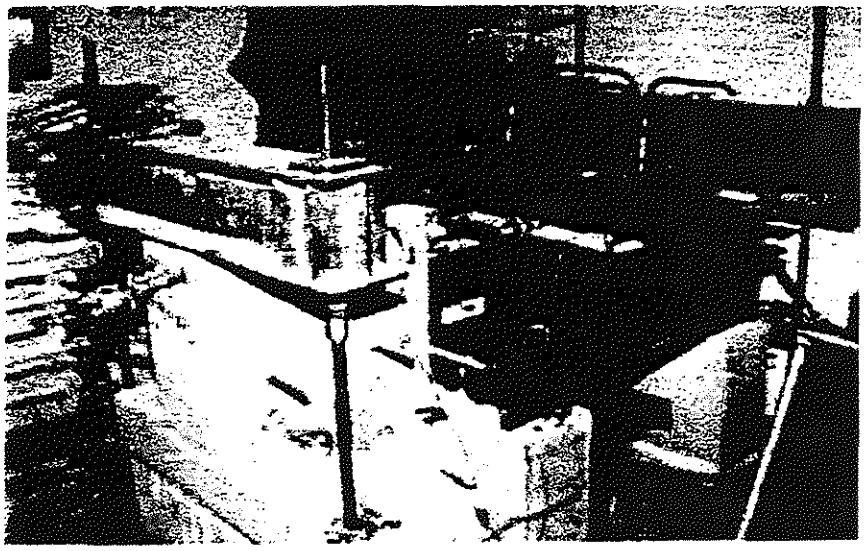

Fig. 1.3-1

As mentioned earlier, there are many variables related to head anchorage behavior investigation. Practically, one of major interest is head maximum anchorage capacity under given concrete strength, and the ratio of head area to bar cross sectional area. In the experiments, the maximum anchorage capacity and load vs. displacement curves were obtained by loading the specimen until failure. Around the head and concrete bearing region, however, the stress distribution and strain variation cannot be easily measured by this type of test; and the interactive relationship between head and concrete cannot be observed visually by conducting pull-out test. Therefore, as a different perspective to the existing research on headed bars, finite element analysis is used to take a closer view inside the specimens through computer generated finite element models. It is expected that through this investigation, useful information will be found about the behavior between the head and concrete in terms of stress distributions, stress concentrations, status of strain variations, and displacements. The models will be based on the work done at Kansas and will be used to help explain the behavior observed during these tests.

CHAPTER 2

Theory And Method

2.1 The Finite Element Method

The finite element method is a numerical procedure for analyzing structures and continua. Usually, the problem addressed is too complicated to be solved satisfactorily by classical analytical methods. The problem addressed in this project is a 3D stress and strain analysis problem which is too difficult to be handled by traditional analytical methods. By using the finite element method with the help of a computer, the procedure produces many simultaneous algebraic equations that must be solved. Results are rarely exact. However, errors can be decreased by processing more equations, and results accurate enough for engineering purposes are obtainable at reasonable cost.

Discretization is a basic finite element concept, that is, the finite element method models a structure as an assemblage of small parts, referred to as elements here. Each element is of simple geometry and, therefore, is easier to analyze than the actual structure. In general, the more elements, the more accurate the results are.

The finite element method also has disadvantages. A finite element analysis cannot provide a closed-form solution for an analytical study of the effects of changing various parameters. Without a computer, a reliable program, and intelligent application, a practical finite element analysis is not feasible. Also, experience and good engineering judgment are needed in order to define a good model for analysis.

2.2 The Computer And Software

During this investigation, Hewlett Packard UNIX workstations are used along with the finite element software, ANSYS5.3, which is a major computer program. The program is capable of creating 2D and 3D models in any geometry shape based on user's skill, experience and time available. There are many linear and nonlinear elements can be chosen from the element library depending on different applications. Also, the loading and boundary conditions are easily controlled by user with the graphical user interface of ANSYS5.3. Although the software is powerful, it is still a challenge for the user to use such a large and complicated program. It requires the user to have a good understanding of fundamental concepts of the finite element method and of program's functions. Computers can only do what the user tells them to do. If input is wrong, then so are the results. So, conducting a finite element analysis is a careful user-computer interface procedure.

2.3 Finite Element Models And Limitations

In the finite element method the close physical resemblance between the actual structure and its finite element model is an important feature that makes a finite element analysis possible. Therefore, the formation of an accurate finite element model for this project is based on the imitation of the experimental beam-end specimen.

No full scale specimen was modeled in this investigation due to limited time, research, and computer resources. All finite element models used in this project were simplified partial models of experimental specimens. The model was cut out from the top portion of a specimen with headed bar included, plus surrounding concrete. From the experience of testing some initial "mock-up" models, it turned out that it was not feasible

to make even a small portion of a full "specimen" work properly. After the number of elements were reduced, the meshes on finite element model were too coarse to make sense. The problem was solved by taking advantage of symmetrical property of specimen, the model employed only half of headed bar and related surrounding concrete, cutting off more concrete volume behind the head, and using different density of mesh within the model depending on intensity of stress concentration. Also, the bond between deformed bar surface and concrete was not modeled due to these reasons: 1) the bar embedded length from the root of head to front face of concrete block is only one foot so its bond effect is minor compared to the bearing capacity of the head; 2) with limited research and understanding, it is difficult to create finite model that reflects the bond effect without large increases in problem size and 3) the area of interest is under the head and by eliminating bond, a conservative solution is obtained.

Both linear and nonlinear models were created during the investigation. For linear models, several preliminary 3D linear models were produced in which there were no relative movements between the head and concrete were used for investigating the general interactive behavior of the head and surrounding concrete. These results will be presented in Chapter 3 of this report. Second, considering boundary conditions between the head and concrete in terms of the relative movements in both lateral and longitudinal directions, a more sophisticated 3D linear model was created and will be discussed in Chapter 4. Lastly, in order to make some comparisons between linear and nonlinear models, a so-called "2D slice" linear model and a "2D slice" nonlinear model were created and are explained in Chapter 5.

There are a great number of variables involved in the analysis and the resulting data during the whole analytical process are complex. Obviously, the relationships among these parameters cause the analysis to be complicated. For this reason, the analysis scope has been simplified so that focusing on the major interest of this observation could be achieved.

In Chapter 3, the so-called path operation which is one of general post processing operations provided by ANSYS is used. By connecting at least two nodes in a model, a path can be created in any direction, and at anywhere within the model. Along a selected path, a variety of variables can be mapped on the path for presentation and further discussion or data processing. By using the path operation, one can examine almost any variable by plotting a curve or making a list along the selected path. Practically, for each model only three typical paths reflect the major interests and were selected in preliminary models. By connecting nodes among a model, Path No.1 is defined on the front face of head that is in contacting with the concrete bearing area. Path No. 2 is on the concrete bearing surface that is under the head in compression and extended to the edge of that bearing surface. Path No.3 also is selected for the observation of concrete, which is perpendicular to Path No. 2.

For the advanced 3D linear model and two slice models which will be discussed in Chapters 4 and 5, respectively, several oblique color plots are used for presentation of the computer results. Since the stress distributions shown on these pictures are color contours this is more effective to give a visual impression of the computer results and make the discussion fast and more effective by using these color plots.

The following chapter will begin the discussion of the preliminary models. Chapters 4 and 5 will follow and will present the balance of the analysis models. The results will show how the loads carried by the head and dissipated by the concrete. Of interest will be the state of stress under the head and how effective the head is in carrying the bar force.

CHAPTER 3

Preliminary Models

Before more advanced finite element model could be created, two groups of preliminary models were tested. The objective of using preliminary models was to observe the head and concrete interactive behavior. It was expected that from the preliminary models the fundamental understanding of how the headed bars were anchored within the concrete so as to identify key aspects for further study.

Like real experimental tests, this "virtual experiment" using the finite element analysis also has its limitations. As mentioned before, the simplified finite element models are not in full scale and the numbers of "specimens" are limited compared to the experiments. So there is no direct comparison between an individual computer model result and an individual experiment result. Although several preliminary models have been employed during preliminary stages of analysis, only the cases that typically represent the intended investigation are reported in this section.

3.1 Introduction to Modeling

All preliminary finite element models presented in this section are 3D linear models. During modeling, 3D global coordinate system was used and both 2D and 3D solid linear finite elements were applied in order to create the solid model. Also, materiel properties for concrete and steel such as Poisson's ratio and the Modules of Elasticity were assigned to the concrete and headed bar elements. At the interface between the head and the concrete, as well as the concrete behind the head, the elements of both steel and concrete share common nodes. This aspect means that there is a perfect connection between the head and the concrete.

Since the finite element model is partial volume of the "specimen" representing half of the specimen, the boundary conditions, therefore, also must represent the proper modeling of the specimen. For the bottom face of the concrete block, restraints in the Y and Z directions are applied to all nodes along that face. Along the surfaces including the headed bar and concrete block that coincide with the symmetrical line, X direction restraints on all nodes also are applied. Because no bond between the bar surface and the concrete has been modeled, additional Y direction restraints are used on a few nodes around the center line of the bar in order to keep the entire headed bar- concrete block model stable as a static structure. Load is applied at the tip of the bar horizontally in the positive Z direction of the global coordinate system. Fig. 3.1-1 conceptually shows the generic model and its loading and constraint conditions.

Generally, models selected here for presentation are similar to each other in many aspects but for the investigation each of them has different features such as different head area, thickness of head, and variation of concrete cover behind the head. For all models, including more advanced models discussed in later chapters of this report, the bar area, A_b, is a constant. That is, the study was a 1" diameter bar corresponding to a No. 8 bar (25 mm) throughout the investigation. The head area, A_t, is 5 A_b and 7.5 A_b with respect to

different model cases, thus there are two groups of models based on head area. Also, there are two types of the head thickness, H_t, of 0.5" and 0.75" used in each group. Moreover, the concrete cover behind the head, H_c, is 0" and 2". Each model is given a specific name for organization purpose. For example, the format of Case212 is a typical name, where numbers 2, 1, 2 stand for model group-2 by head area (A_t =7.5 A_b), type-1 of head thickness (0.5"), and 2" concrete cover behind head, respectively. Detailed discussions about the preliminary models and results will be presented in the following sections.

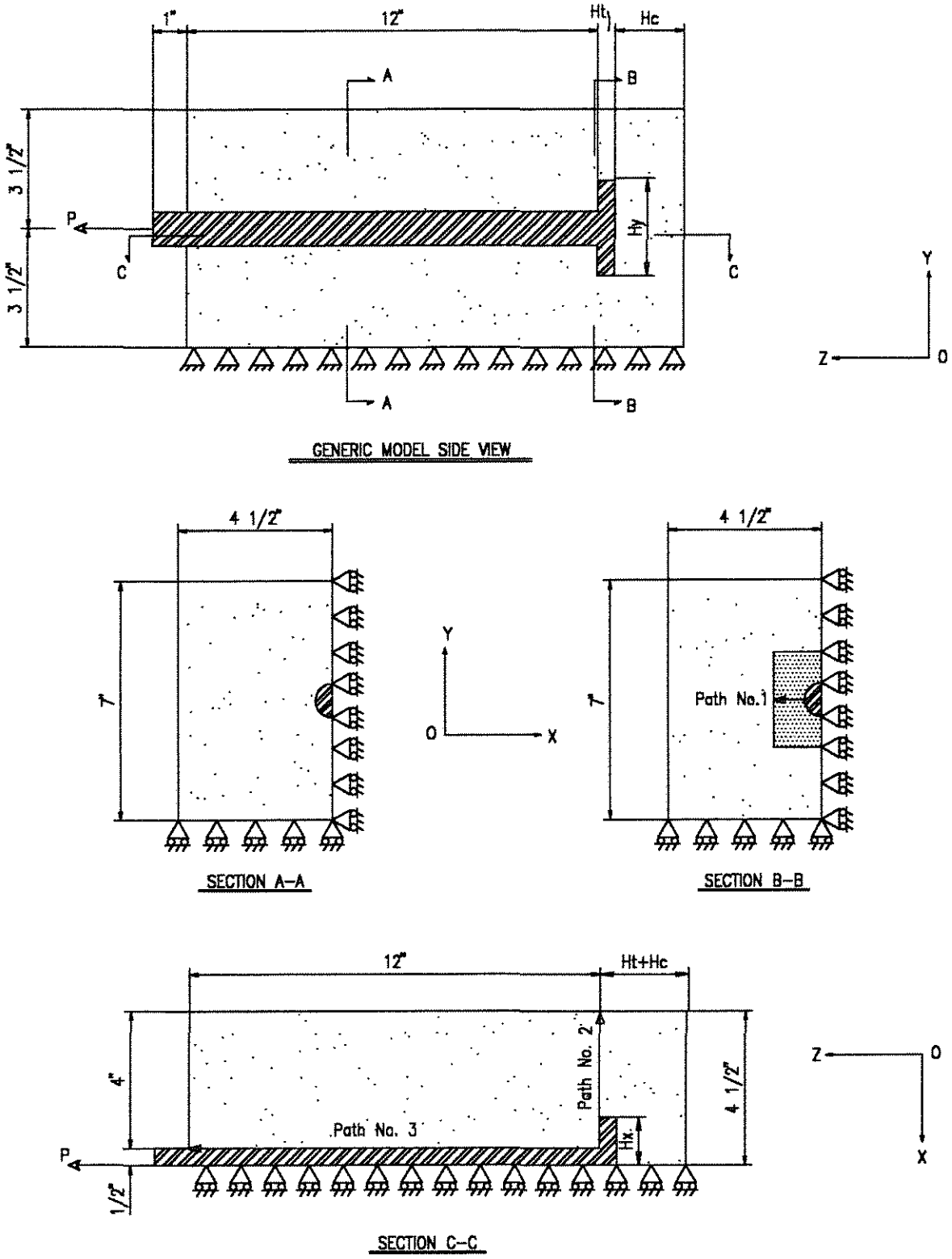
1"
12"
Ht
Hc
A
B
3 1/2"
3 1/2"
P
C
Hy
C
Y
Z
O
A
B
GENERIC MODEL SIDE VIEW
4 1/2"
7"
Y
O
X
SECTION A-A
4 1/2"
7"
Path No.1
SECTION B-B
12"
Ht+Hc
4"
Path No. 2
Path No. 3
Hx
4 1/2"
P
1/2"
Z
O
X
SECTION C-C

Fig. 3.1-1

3.2 CASE110

As the name of CASE110 indicates, the head area used in this model is taken as five times the bar area (actually only half bar and head are modeled by taking advantage of symmetrical property of "specimen") and the head thickness is half inch. Since this is the first trial of the 3D model, for the reason of simplification, there is no concrete cover behind the head considered.

Finite elements selected from the ANSYS5.3 element library are solid-42 with 4 nodes and solid-45 with 8 nodes. Element 42 is mainly employed as an assistance to building the 3D solid model with solid 45 elements during modeling procedure and element 42 is usually unselected before a solution will be executed. For concrete, a Poisson's ratio of 0.2 and a Modules of Elasticity of 3.6×10^6 psi are used, based on the assumption of a 4000 psi compression strength. For steel, a Poisson's ratio of 0.3 and a Modules of Elasticity of 29.0×10^6 psi are assumed.

There are three load levels used in the analysis of this model even though this is a linear load case. The purpose of doing so is to see the variation of relative stress concentration under different load levels. The head deformation, obviously, is proportional to load level but the different degree of deformed surface of the head effects the stress distribution on concrete bearing surface, though it is only minor difference. According to experimental results, the maximum applied load that a typical specimen could hold is about 36 kips, so it can be assumed that the stress on the bar is still under the yield point when the specimen reaches ultimate capacity. Generally, it could assumed that the concrete bearing strength underneath the head controls the specimen capacity. The degree of stress concentration on that bearing surface is a key factor to the bearing strength under a given ratio of head to bar areas. In Case110, as well as the rest of preliminary models, the three load levels are: P1= 5,890 lb., P2=11,780 lb., and P3= 17,670 lb., which are equivalent to the nominal stress levels of 15000 psi, 30000 psi, and 45000 psi on the bar cross section, respectively.

The major input parameters for Case110 are listed below:

Input Parameters for CASE110

Item	Value	Remark
1. Finite Elements:		
concrete and steel	ANSYS solid 42	(4 node element)
concrete and steel	ANSYS solid 45	(8 node element)
2. Modules of Elasticity:		
steel	$E_s = 29.0 \times 10^6$ psi	
concrete	$E_c = 3.6 \times 10^6$ psi	
3. Poisson's ratio:		
steel	$\mu_s = 0.3$	
concrete	$\mu_c = 0.2$	
4. Geometry:		
bar diameter	$d_b = 1$ in	
bar area	$A_b = 0.785$ in^2	
head thickness	$H_t = 0.5$ in	
head area	$A_t = 3.925$ in^2	($A_t = 5 \times A_b$)
long edge of head	$H_y = 1.98$ in	($H_y = \sqrt{A_t}$)
short edge of head	$H_x = 0.99$ in	($H_x = H_y/2$)
cover behind head	$H_c = 0$ in	
5. Loads:		
P1	5,890 lb.	($P1 = 0.5 \times 15000 \times A_b$)
P2	11,780 lb.	($P1 = 0.5 \times 30000 \times A_b$)
P3	17,670 lb.	($P1 = 0.5 \times 45000 \times A_b$)

See Fig. 3.1-1 for more reference information

The results from the solution for this model are presented in following plots and discussion. As expected, along the selected Paths No.1, No.2 and No.3 (see Fig. 3.1-1 for Path locations) the general deformation of the head and the concrete, stress and strain distributions indicate the linear behavior of this finite element model.

Under the applied loads, the head behaves as a cantilevered plate in two-way bending. In this case no concrete behind the head is modeled so that there is no restraint against plate deformation away from the concrete behind the head. By mapping the variable of displacement in the Z direction (UZ) along Path No.1, a plot indicating the displacements along Path No.1 is obtained as shown in Fig. 3.2-1. the three curves in the plot show displacement variations along Path No.1 under the three different load levels, and at the same time they display the deformed outline of the front face of the head. Generally, the overall displacements are small and the slope of each curve increases with respect to the load level. For each load level, the displacement reaches the maximum value at the root of T-head and decreases along the path down to the edge of the head. (global coordinate system)The behavior of the head is similar to a base plate under a column with the difference here being the loading direction. In order to have reference values for studying the stress distributions on the heads and concrete bearing areas in terms of stress concentrations along the selected paths, three normal stresses in the Z direction (SZ) are assumed as SZ1 = 1876 psi, SZ2 = 3752 psi, and SZ3 = 5628 psi from load levels P1, P2, and P3, respectively. These are obtained by using an idealized situation in which the head is stiff enough and concrete is strong enough so that they are in a perfect contact at interface. For calculations of the reference nominal stress, divide each load level by a nominal effective head contact area (A_{te}) which is defined as the head area minor the bar area, that is,

$$SZ_n = P_n / A_{te}$$

$$A_{te} = A_t - A_b \quad (in^2)$$

where SZ_n = Nominal stress (psi)

P_n = Applied load (lb.)

n = 1, 2, 3

Displacement (UZ) Vs. Distance Along Path No.1 for Case110

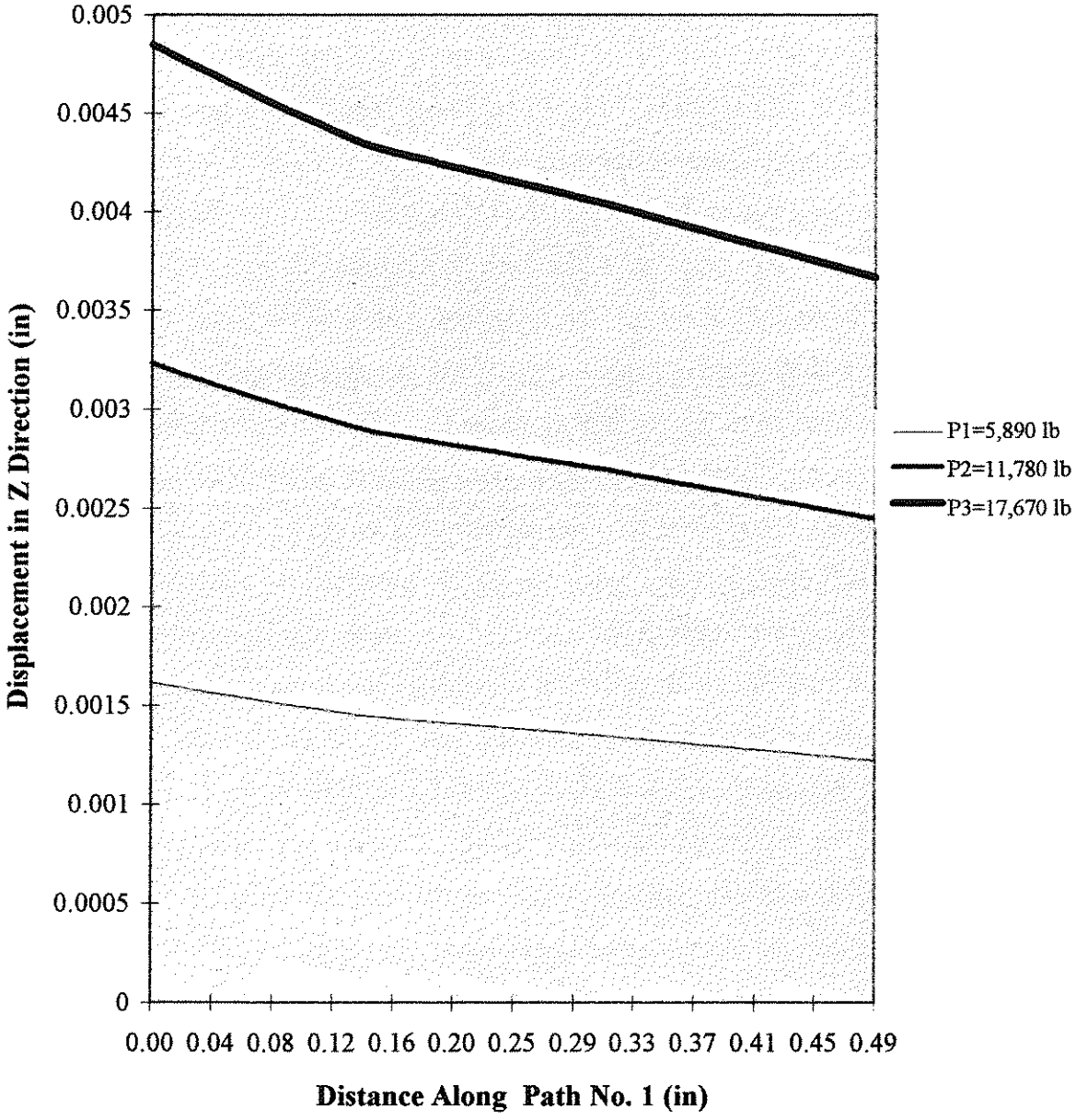

Fig. 3.2-1

For the head, the stress distributions on Path No.1 in the Z direction (SZ) is shown in Fig. 3.2-2. From Fig. 3.2-2 it can be seen that the normal stress (SZ) is not distributed evenly across the head, and tension stress appears within a distance that starts from the root of T-head to 1/4 or 1/3 of the total path length. This situation also appears in the other preliminary models. The strain variation is basically proportional to stress distribution due to model's linear behavior.

For getting a simple visual view of the stress (SZ) concentration factor on the head, Fig. 3.2-3 is used to show the normal stress concentration factor variations along Path No.1. Since this is linear condition, the stress concentration factors on the head are basically same in the three different load levels. The average compressive stress concentration factor can be considered as the normal compressive stress concentration factor on the front face of the head. It varies from 1.0 to 2.76. Therefore, if the ratio of head area to bar area is 5 (A_t = 5 A_b), the maximum compressive stress concentration factor on front face of the head might be considered to be 2.76 for linear conditions, or for the situation where the applied stress level is low with respect to concrete strength.

As expected the headed bar structural behavior is similar to a two-way plate in bending. Although the front face of the head is mainly in contact with the concrete, it is subjected to bending and the strength is basically controlled by the principal stress (S1). This behavior is shown by the principal stress (S1) distribution along the Path No.1 in Fig. 3.2-4. From the plot it can be seen that the maximum principal stress is below 40,000 psi even when a high nominal compressive stress SZ3 of 5678 psi is applied in this case. The principal stress is well below the reinforcing bar yield strength of 60,000 psi. From this point of view, if the small ratio of head area to bar area is used in application, it is likely that the head reinforcement strength will not be a concern, but rather the concrete bearing strength under the compression stresses induced by the head will control.

Stress (SZ) Vs. Distance Along Path No. 1 for Case110

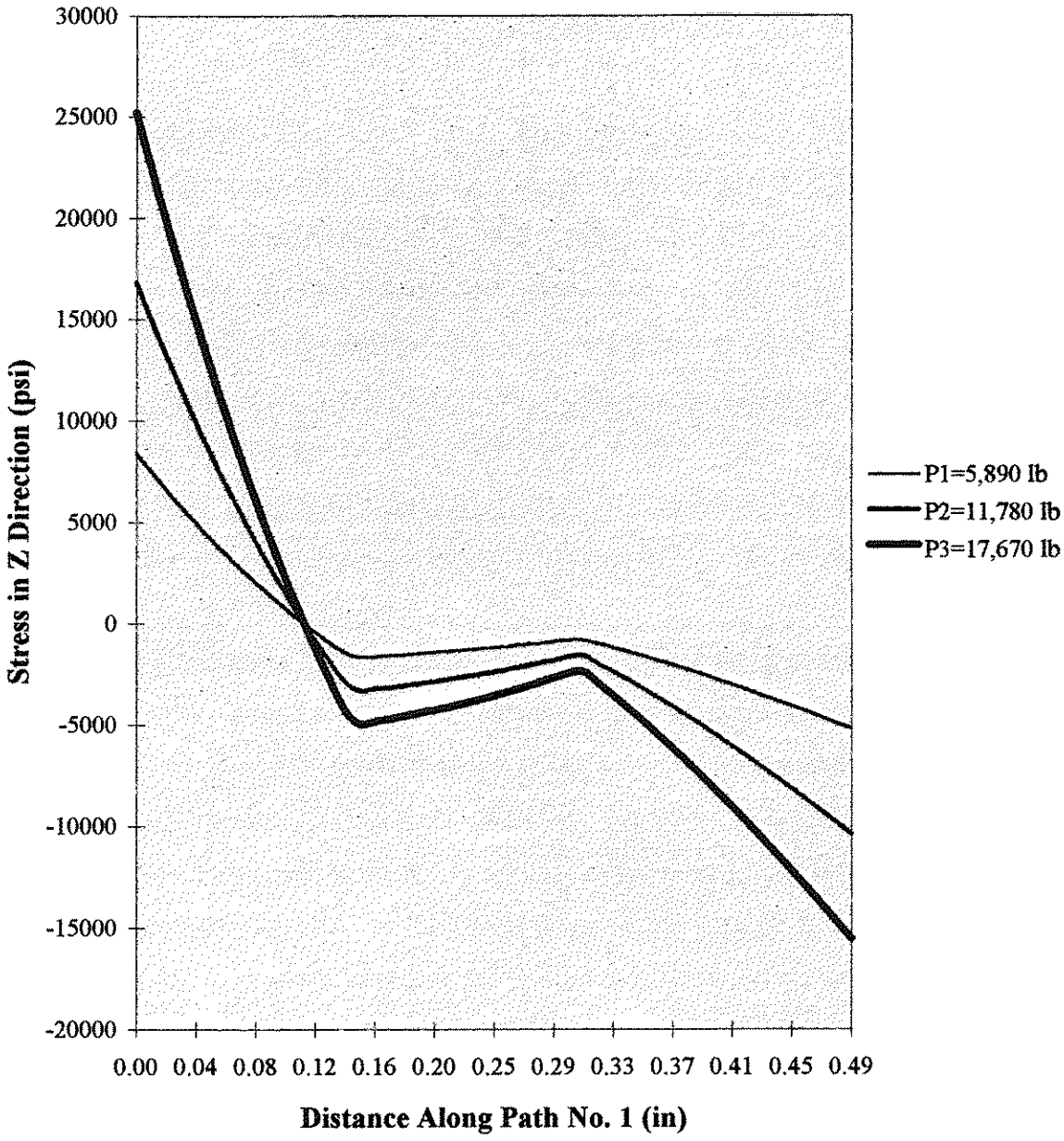

Fig. 3.2-2

Stress (SZ) Concentration Factor Along Path No.1 for Case110

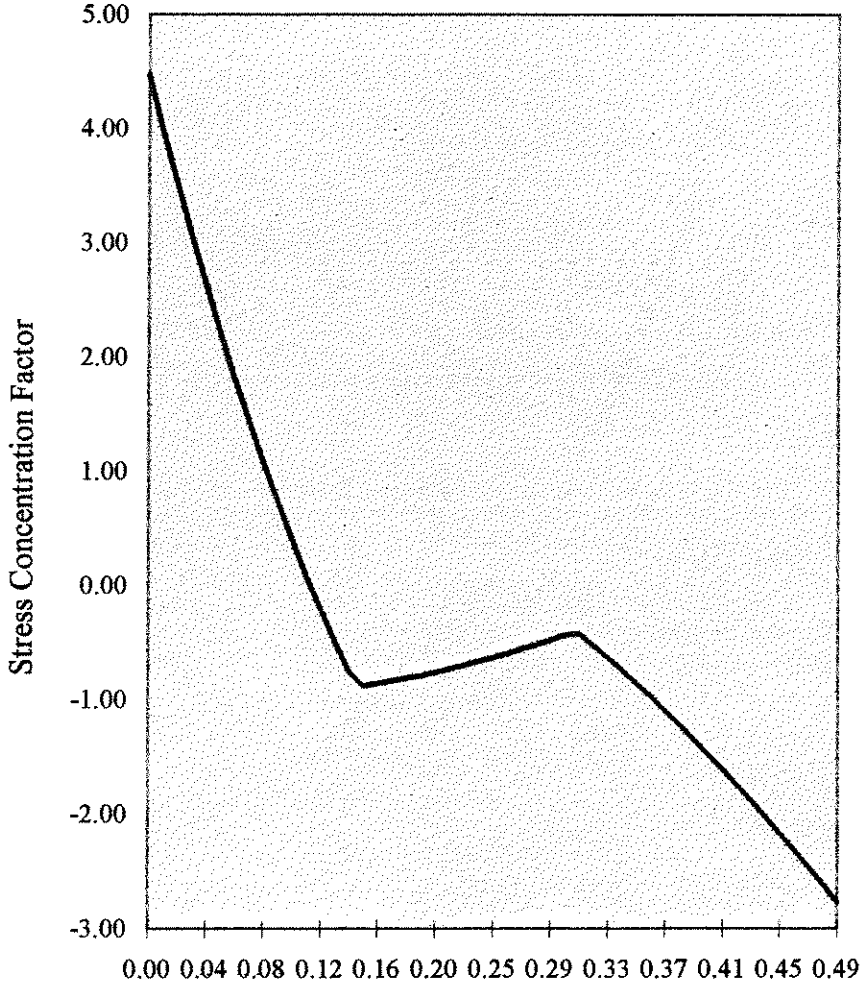

Fig. 3.2-3

Stress (S1) vs. Distance Along Path No. 1 for Case110

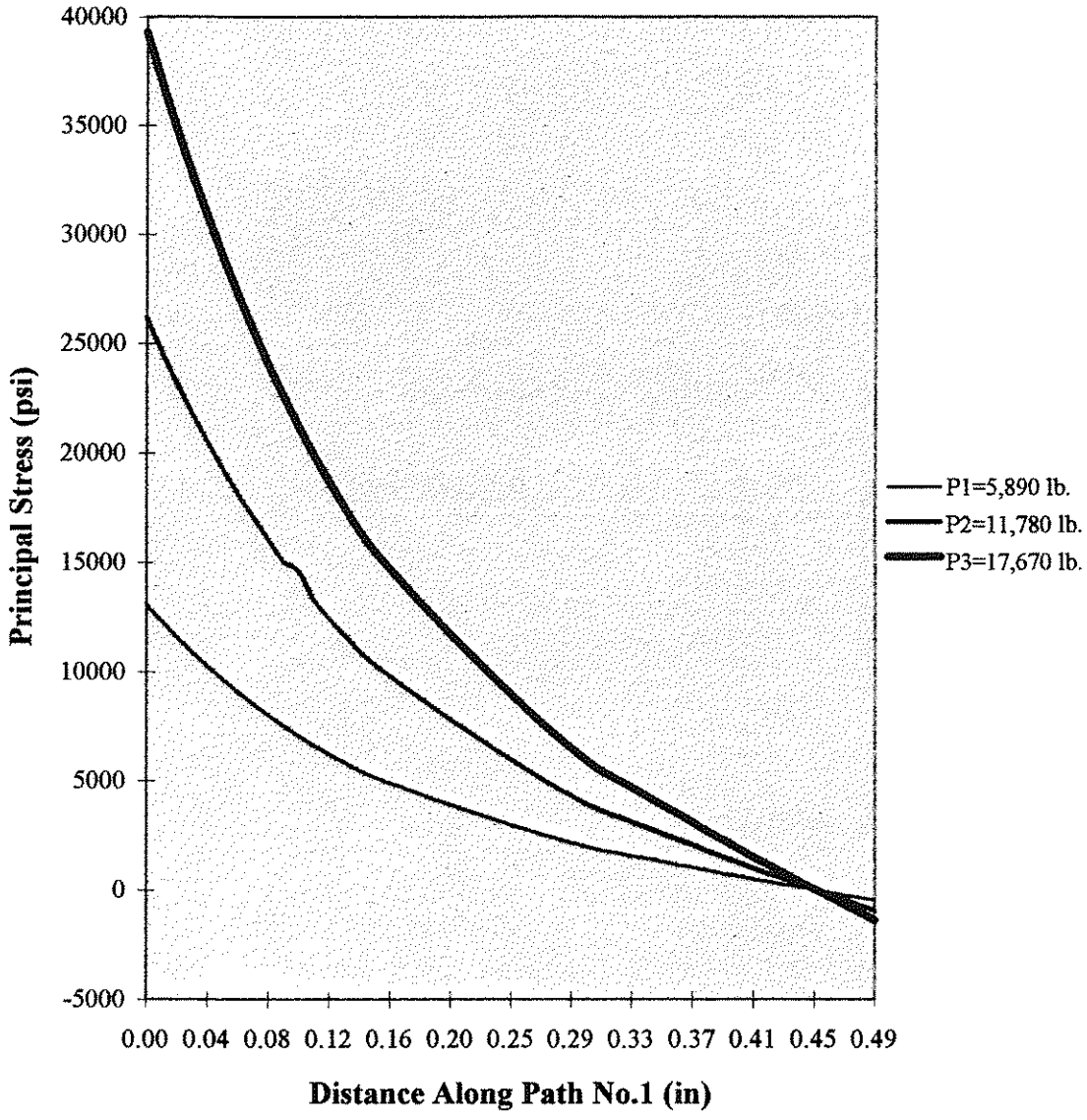

Fig. 3.2-4

For investigation of the concrete behavior, two paths are selected. First, Path No.2 is used to observe the stress and strain status of concrete that is directly under the head to evaluate the compression here and in the nearby area. Path No.2 starts at a point that coincides with the starting point of Path No.1 at the edge of the reinforcing bar where it joins the head. This path direction is parallel to Path No.1 but on the concrete side and ends at the edge of cross section. Path No. 3 basically begins at the same starting point as Path No.2 in the direction parallel to bar and ends at the front face of concrete specimen, so the stress and strain variation along that path also can be investigated.

By mapping the stress along Path No.2, it can be seen that how the normal compressive stress (SZ) distribution on the cross section of concrete under the head and in the vicinity varies, Fig. 3.2-5. For each load level the maximum compressive stress occurs at point where the path starts at the bar-head intersection and decreases proportionally to the distance away from the starting point of Path No.2. At the point where it is approximately meets the edge of the head, there is a sharp transition in stress distribution due to release of compressive force from the head. On the area outside of the head compression region, the stress level is low and could be ignored. Conceptually, the concrete under the head behavior like soil under a spread footing in a building. From the plot it can be observed that the stress level in compressive in the concrete under the head is high, especially in load level P3. The stress reaches a level greater than 10,000 psi due to the assumed linear condition. So in reality this high a stress should already have caused the 4,000 psi strength concrete around that stressed area to fail. Of course it is to be expected that this stress would redistribute and a new balance provide to avoid structural failure.

The average stress concentration factor variation along the concrete bearing face in this case is shown in Fig. 3.2-6. The factor varies from -1.07 to -1.86 over the concrete under the head. If the ratio of head area to bar area is 5 ($A_t = 5\ A_b$) and the head thickness is 0.5 inch, the maximum compressive stress concentration factor might be considered as 1.86 for a linear condition based on the maximum value obtained in this analysis.

Stress (SZ) vs. Displacement Along Path No. 2 for Case110

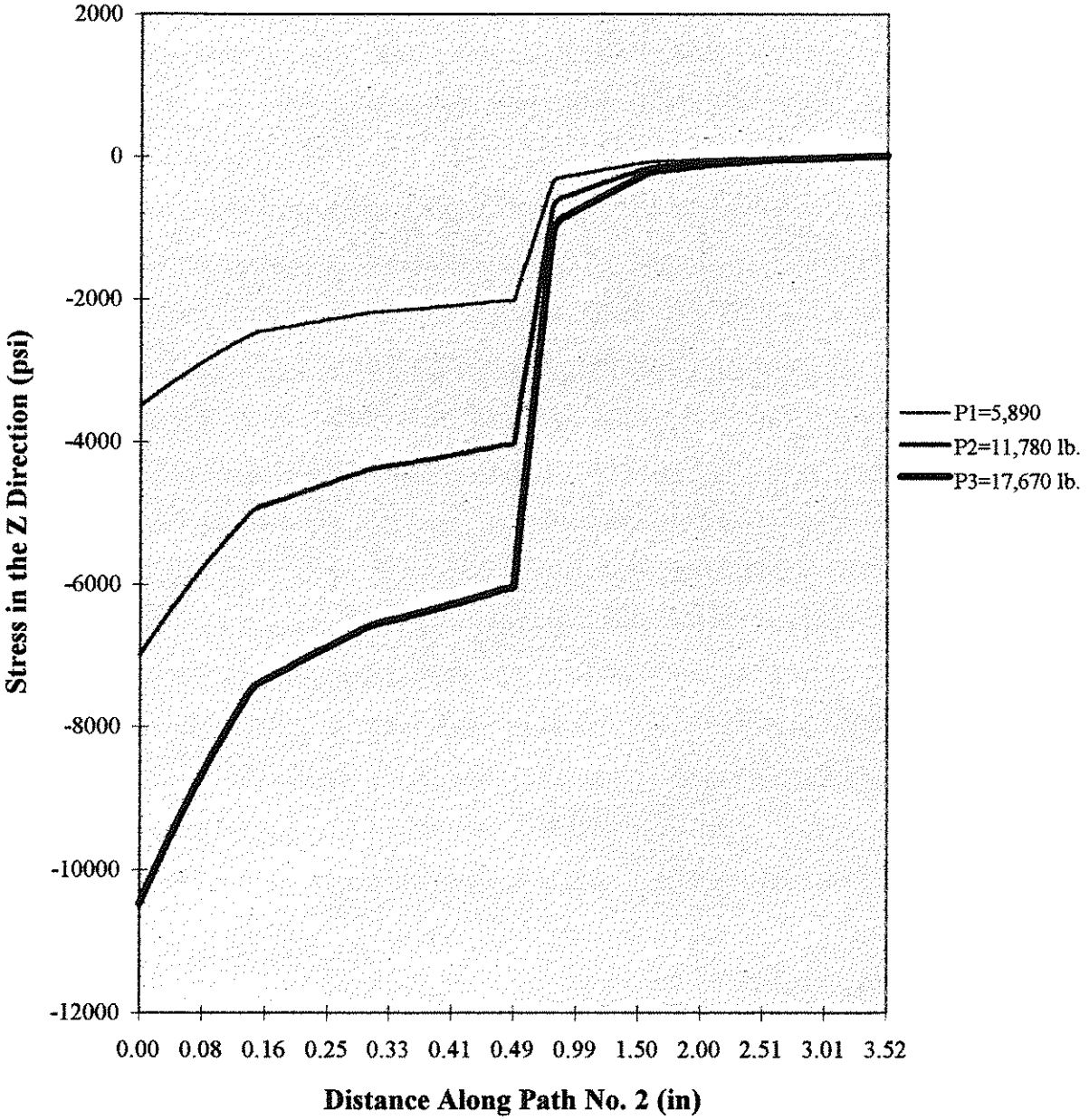

Fig. 3.2-5

Stress (SZ) Concentration Factor vs. Distance Along Partial Path No.2 for Case110

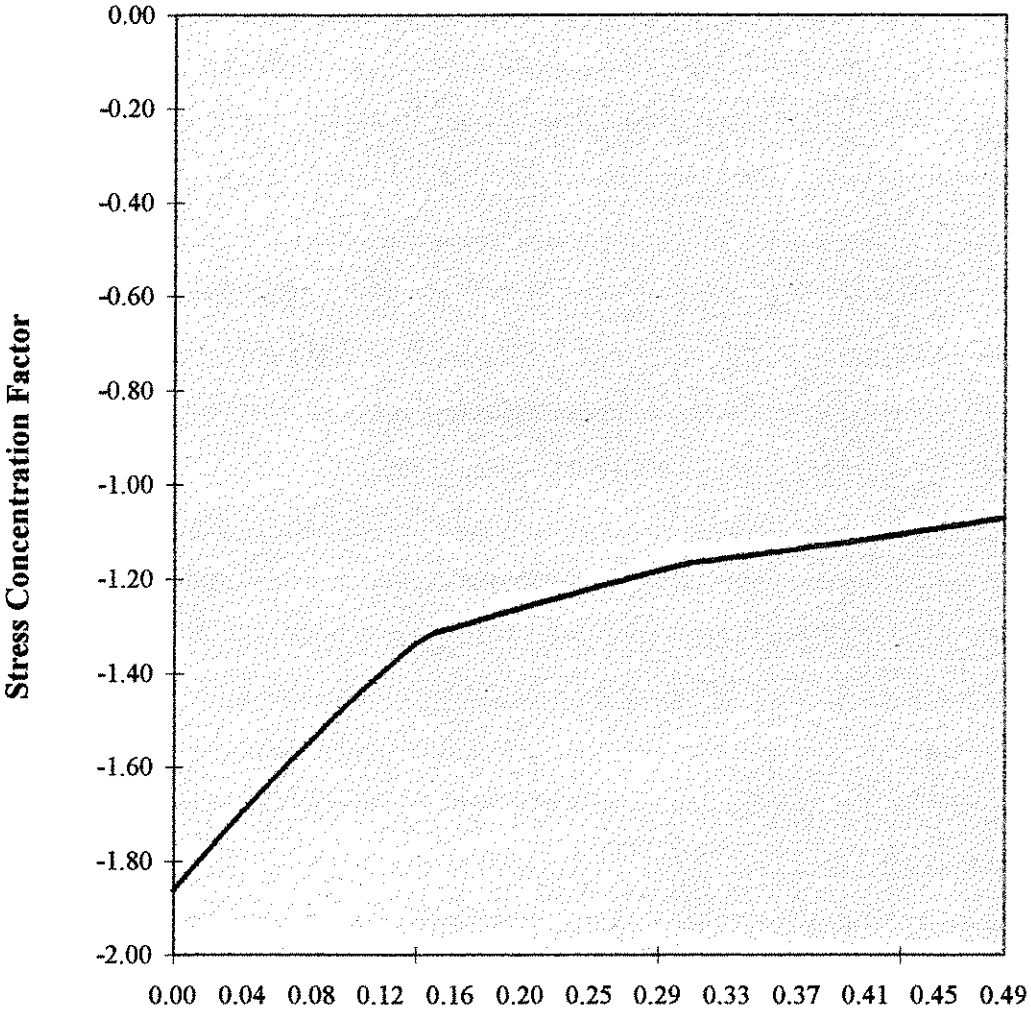

Fig. 3.2-6

For a normal density concrete under a compressive test, a strain of 0.003 (in/in) is usually the maximum value allowed for design. If the strain exceeds this value, the concrete strength should be considered as in a failure situation. The strain distributions over the concrete bearing area is shown in Fig. 3.2-7. The strain variation patterns basically match the stress distributions on the same Path No.2 as expected. The maximum value appears at beginning point of the path at the bar-head junction and decreases along the path down to the point where it matches the edge of head like stress distribution behavior in the same way. It is interesting to see that maximum strain at load level P3 reaches a value about 0.0024 (in/in) which is close to 0.003 (in/in) meanwhile the corresponding stress (see Fig. 3.2-5) is over 10,000 psi. Admittedly, this is because of model's linear behavior, it might imply that there is over stressed concrete, however, in reality, due to confinement around the head-concrete region of 3D solid structure, the distribution will be different than this predicted value.

As mentioned before, concrete bearing capability loss is one typical failure of this type structure. It also is interesting to see that a shear capacity failure could occur prior to concrete bearing capacity loss. In Fig. 3.2-8, the principal stress along the Path No.2 is plotted. From the plot it is seen that the concrete directly under the head is subjected to compressive stress because the principal stress (S1) indicated in that region is all compressive stresses. However, within the distance from the point matching the edge of head to a point about one inch, the principal stresses change abruptly from compressive stress to zero and then to tensile stress. At the peak points of tensile stresses, a middle value of 500 psi in tension occurs. It would be expected that it is the tension principal stress that causes concrete around the edge of head to crack.

Path No.2 is used to investigate the concrete that lies immediately under the head while Path No.3 is selected to observe the stress and strain variations within the concrete in longitudinal direction along the bar axis. The starting point of Path No.3 is not exactly

Strain (EZ) vs. Distance Along Path No. 2 for Case110

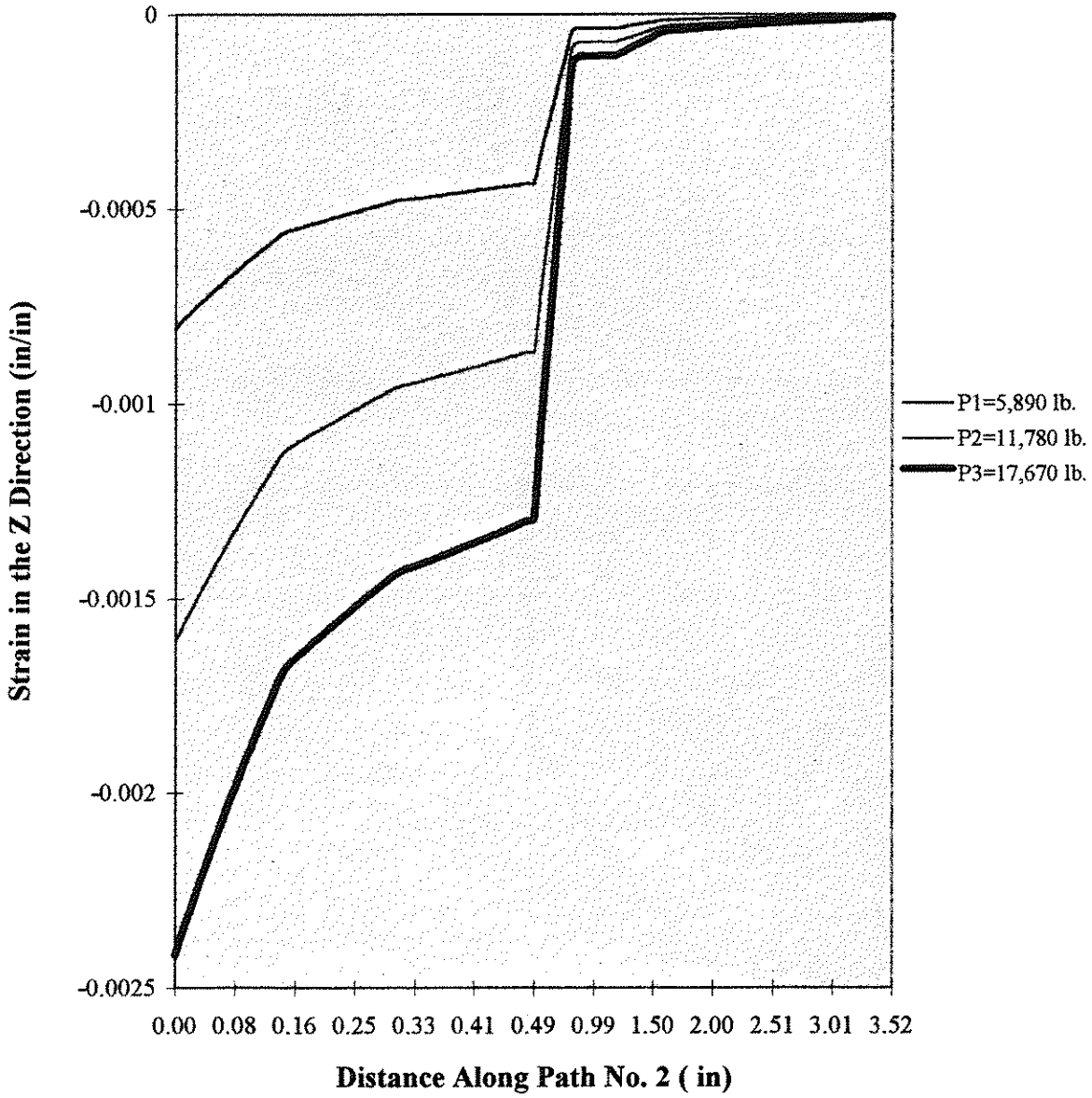

Fig. 3.2-7

Principal Stress (S1) vs. Distance Along Path No. 2 for Case110

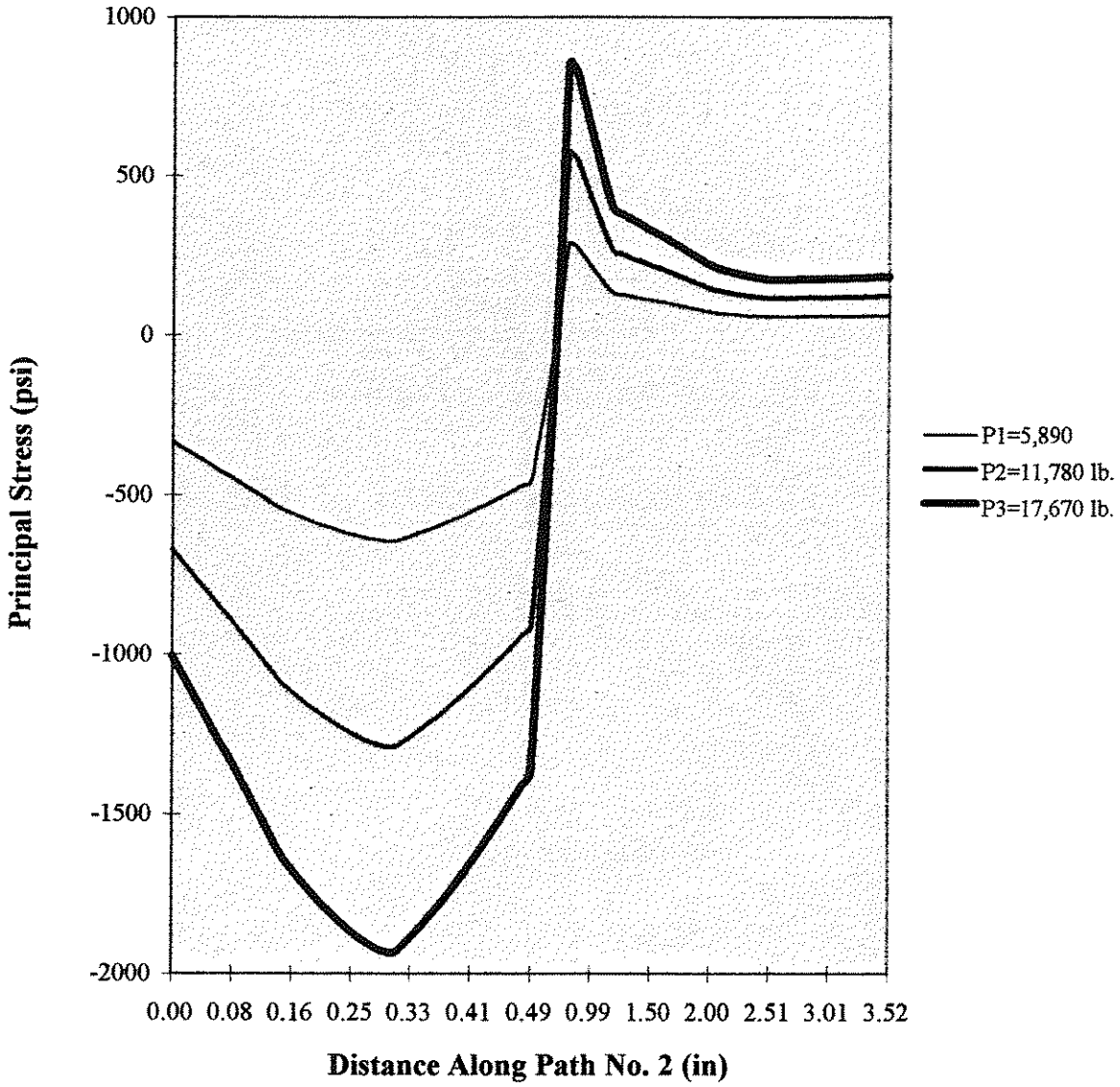

Fig. 3.2-8

at the same point as Path No.2 due to operational selection during post-processing of computer results but is very close. The stress and strain variations are displayed in Fig. 3.2-9 and Fig. 3.2-11, respectively. The purpose of investigating stress and strain distributions on Path No.3 is to find out how the stress and strain decreases along Path No.3 and how far away the influence of the head is seen in the longitudinal direction.

Due to limited results, the stress and strain in the Z direction are selected for discussion only. In Fig. 3.2-9 it can be observed that for each load level the stress (SZ) is compressive and that the maximum value appears at a point immediately under the head. The stress decreases quickly from the starting point to a point about 4 in. away from the head. After that, the stress continues to reduce and beyond 6 in. away from the head the stress level is low and declines essentially a value that can be ignored.

From the above information it could be assumed that if the stress level in the concrete under the head is too high, then localized concrete crushing will occur. Therefore, the following situations might be possible depending on overall stress level and confinement: 1) the stress redistribution could be expected and stress and strain influence along the depth could continue, 2) the stress level is too high and surrounding concrete is not strong enough to offer sufficient confinement; the concrete crushing action could continue, meanwhile the stress and strain influence curve as shown would continue, and the structure could fail either due to large displacement or cracking. From these results, in the application of headed reinforcement confining reinforcement in front of the head within 6 inches of the head to enhance the performance is recommended. Moreover, the confinement is most effective in this region immediately in front of the head and its effectiveness is reduced with distance away form the head. This behavior also was noted by Wright and McCabe (1997) in their experimental study.

Stress (SZ) vs. Distance Along Path. No. 3 for Case110

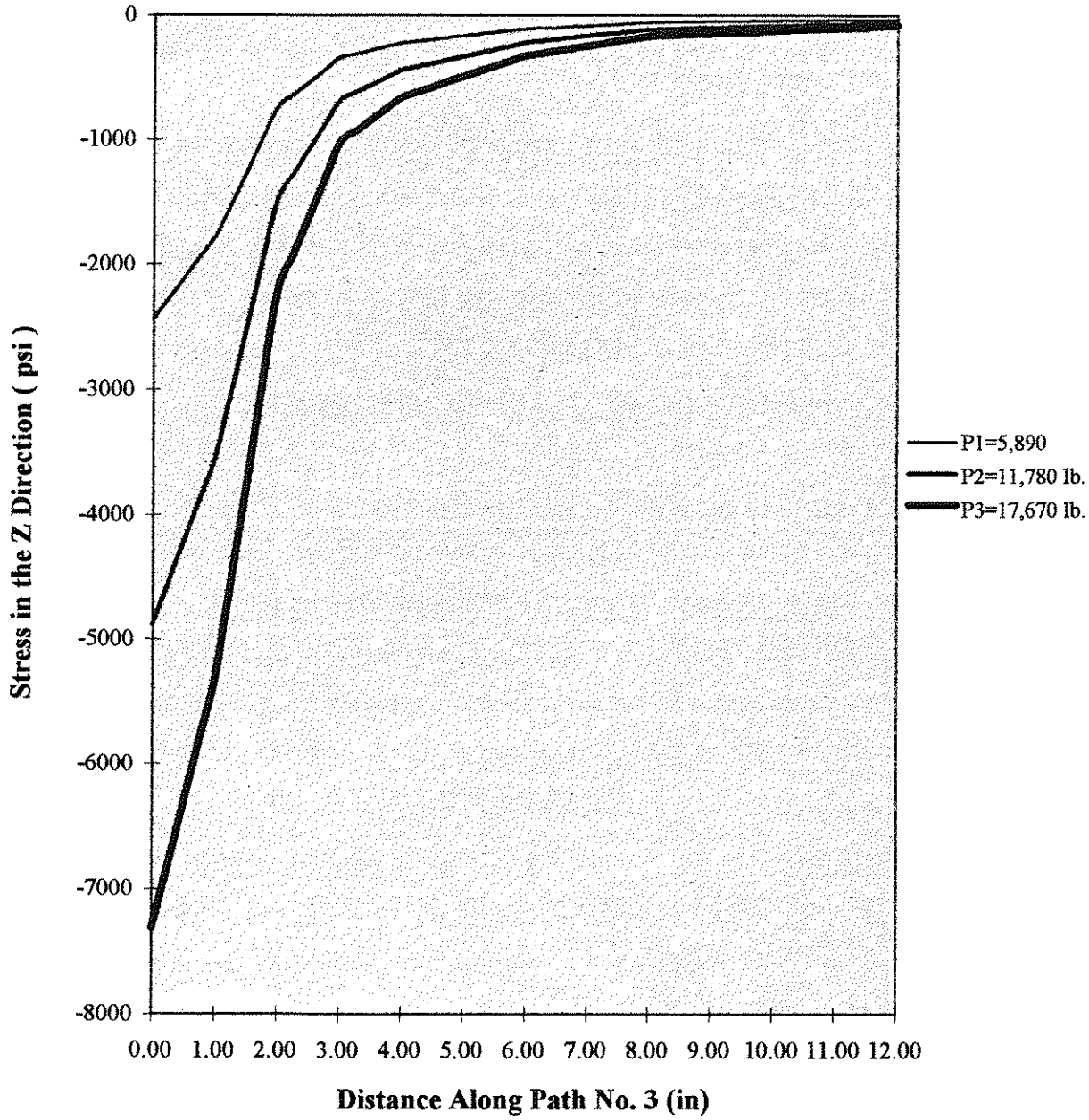

Fig. 3.2-9

3.3 CASE112

The purpose of using model Case112 is to form some comparisons between the models in Case110 and Case112. Generally, both models are the same. The only difference between these two is the addition of concrete cover behind head in Case112 but not in Case110. The concrete cover behind the head (H_c) used in this model is 2 in. (see "Input Parameters For Case112" on the following page.) This case is intended to investigate the influence of concrete cover behind head to see how it influences the head-concrete behavior with respect to stress distribution over the head and adjacent concrete bearing area. The addition of cover also corresponds to typical design practice where coverage of the reinforcement is required by the ACI building code.

As expected there are indeed some interesting results revealed in this model. For the head, the normal stress (SZ) distribution is primarily the same as in Case110 but the stress concentration factor varies in a different manner. As shown in Fig. 3.3-1, the average stress concentration factor changes from -3.78 to +4.47. The stress concentration factor within a distance from the starting point of the path to the point about 2/3 of the length of the path is basically the same as Case110, while the factor increases in absolute value within the rest of Path No.1. This situation is caused by the concrete cover behind the head providing resistance for the head against backward deformation near its edge. The back face of the head in Case110 is not confined by the concrete so that the head is more flexible compared to Case112. Here the head is subjected to the restraint from the concrete cover behind the head and so the deformation action is reduced.

Skipping the tensile stress part, the stress concentration factor in this model is within the range of -1.0 to -3.78. Compared to the values of -1.0 to -2.78 in Case110, the maximum stress concentration factor in Case112 is about 1.3 times as high as in Case110. This behavior is mainly caused by the normal stress level increasing in part of the head, which is a strip area of about 1/6 of the width of the head by its length. It also is

interesting to observe that the stress increment in this partial area on the head also decreases the stress level in the concrete bearing area (to be discussed later). The major input parameters for Case112 are listed below:

Input Parameters for CASE112

Item	Value	Remark
1. Finite Elements:		
concrete and steel	ANSYS solid 42	(4 node element)
concrete and steel	ANSYS solid 45	(8 node element)
2. Modules of Elasticity:		
steel	$E_s = 29.0 \times 10^6$ psi	
concrete	$E_c = 3.6 \times 10^6$ psi	
3. Poisson's ratio:		
steel	$\mu_s = 0.3$	
concrete	$\mu_c = 0.2$	
4. Geometry:		
bar diameter	$d_b = 1$ in	
bar area	$A_b = 0.785$ in^2	
head thickness	$H_t = 0.5$ in	
head area	$A_t = 3.925$ in^2	($A_t = 5 \times A_b$)
long edge of head	$H_y = 1.98$ in	($H_y = \sqrt{At}$)
short edge of head	$H_x = 0.99$ in	($H_x = H_y/2$)
cover behind head	$H_c = 2$ in	
5. Loads:		
P1	5,890 lb.	($P1 = 0.5 \times 15000 \times A_b$)
P2	11,780 lb.	($P1 = 0.5 \times 30000 \times A_b$)
P3	17,670 lb.	($P1 = 0.5 \times 45000 \times A_b$)

Stress (SZ) Concentration Factor vs. Distance Along Path No.1 for Case112

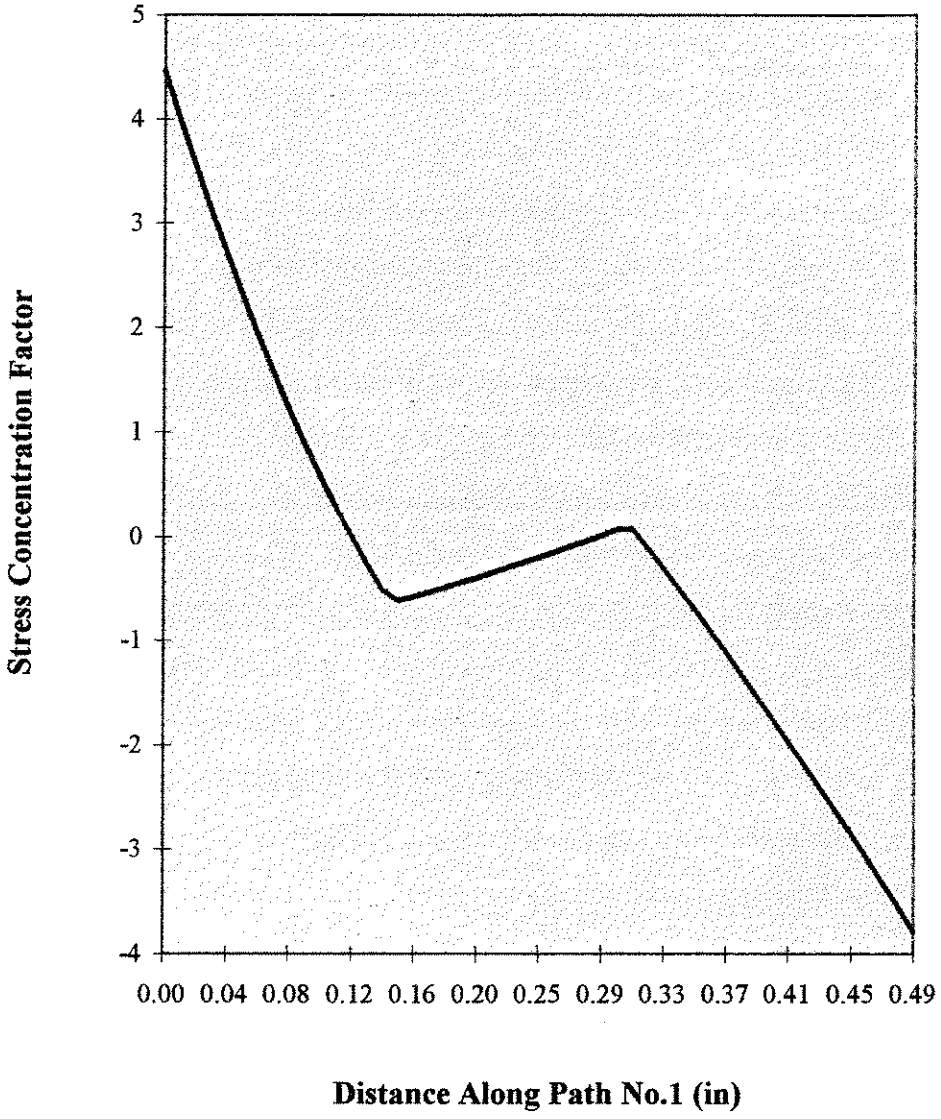

Fig. 3.3-1

As a result of adding concrete cover behind the head, the stress (SZ) level over the concrete bearing area is reduced and the variation of stress concentration factor also reflects the change in stress distribution.

By comparing the both Case110 and Case112 though Fig. 3.2-5 and Fig. 3.3-2 , It can be observed that overall stress level in Case112 is lower than that in Case110. Taking the stress variation curves at load level P2 in both cases for an example, the maximum compressive stress reaches a level of about -7000 psi in Case110 while in Case112 it is reduced to -5600 psi. The stress concentration factor variation along the partial Path No.2 in Case112 is shown in Fig. 3.3-3. It varies from -0.73 to -1.57, whereas it changes from -1.07 to -1.86 in Case110. Therefore, the stress concentration factor over the concrete bearing face is reduced, while the stress concentration factor is increased in the head because of existence of concrete behind the head as mentioned before. This behavior implies that the confinement from the concrete cover behind head increases the effective stiffness of the head and that the concrete behind the head develops a compressive stress in action against backward movement of the head. In Case110, there is no restraint against head movement behind the head so only the concrete bearing area that is in contact with the head's front face carries the compression force from the head. Thus, the slight backward deformation of the head reduces the contact area in Case110. However in Case112, the concrete cover behind the head provides restraint against head deformation away from the load point when loaded. Therefore, in Case112 not only is the concrete in front of the head active but also the concrete behind the head acts to provide a reaction to head deformation. This restraint helps the head flat and increases the contact area.

The stress reduction in the longitudinal direction also is found along Path No.3 in Case112 due to the addition of concrete cover behind the head. Based on the comparison between the results from Case110 and Case112, shown in Figs. 3.2-10 and 3.3-4, respectably, the stress distribution behavior in these two cases basically can be seen to the same. However, the stress value is reduced in Case112 compared to that in Case110. For

Stress (SZ) vs. Distance Along Path No. 2 for Case112

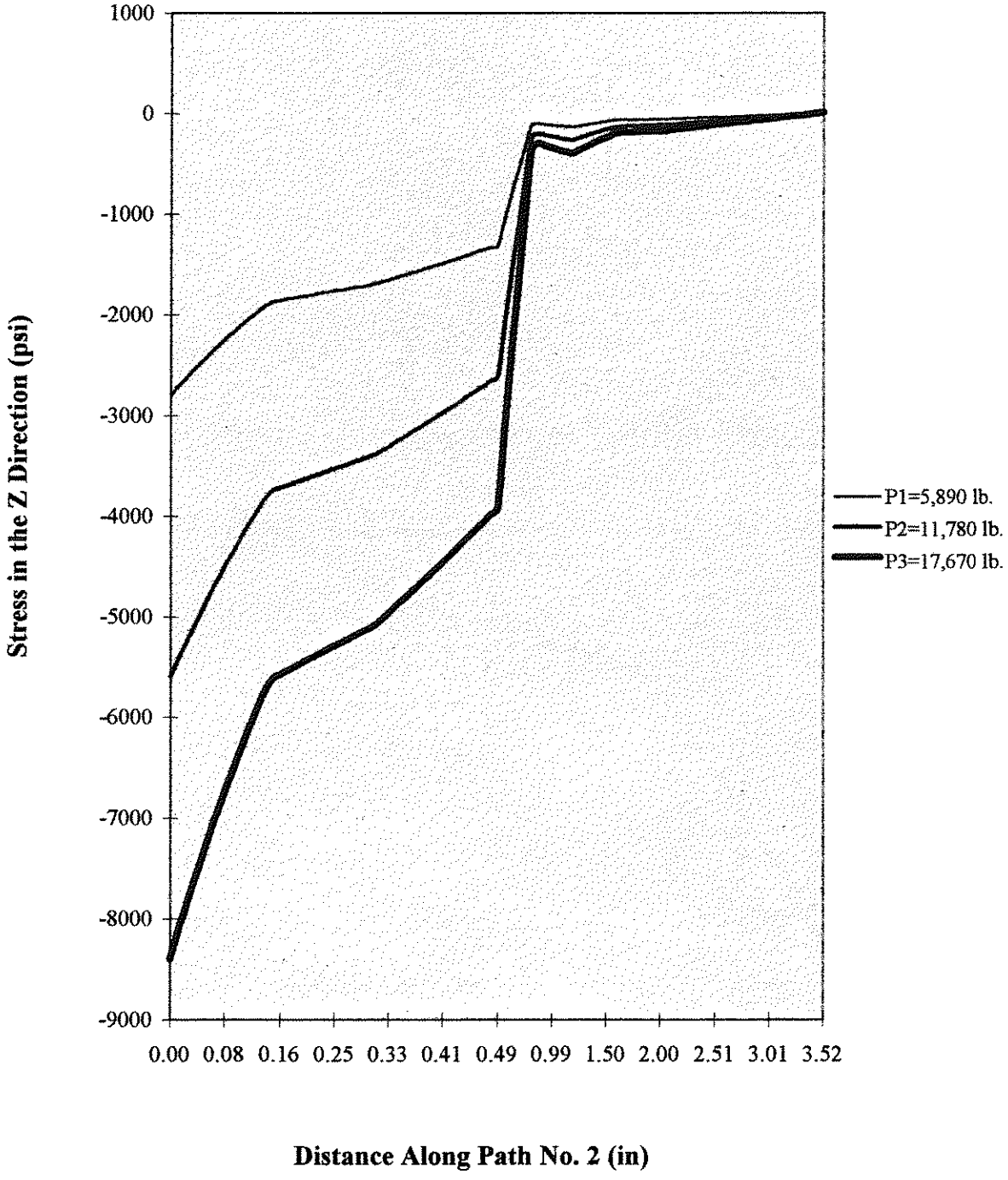

Fig. 3.3-2

Stress (SZ) Concentration Factor vs. Distance Along Partcial Path No.2 for Case112

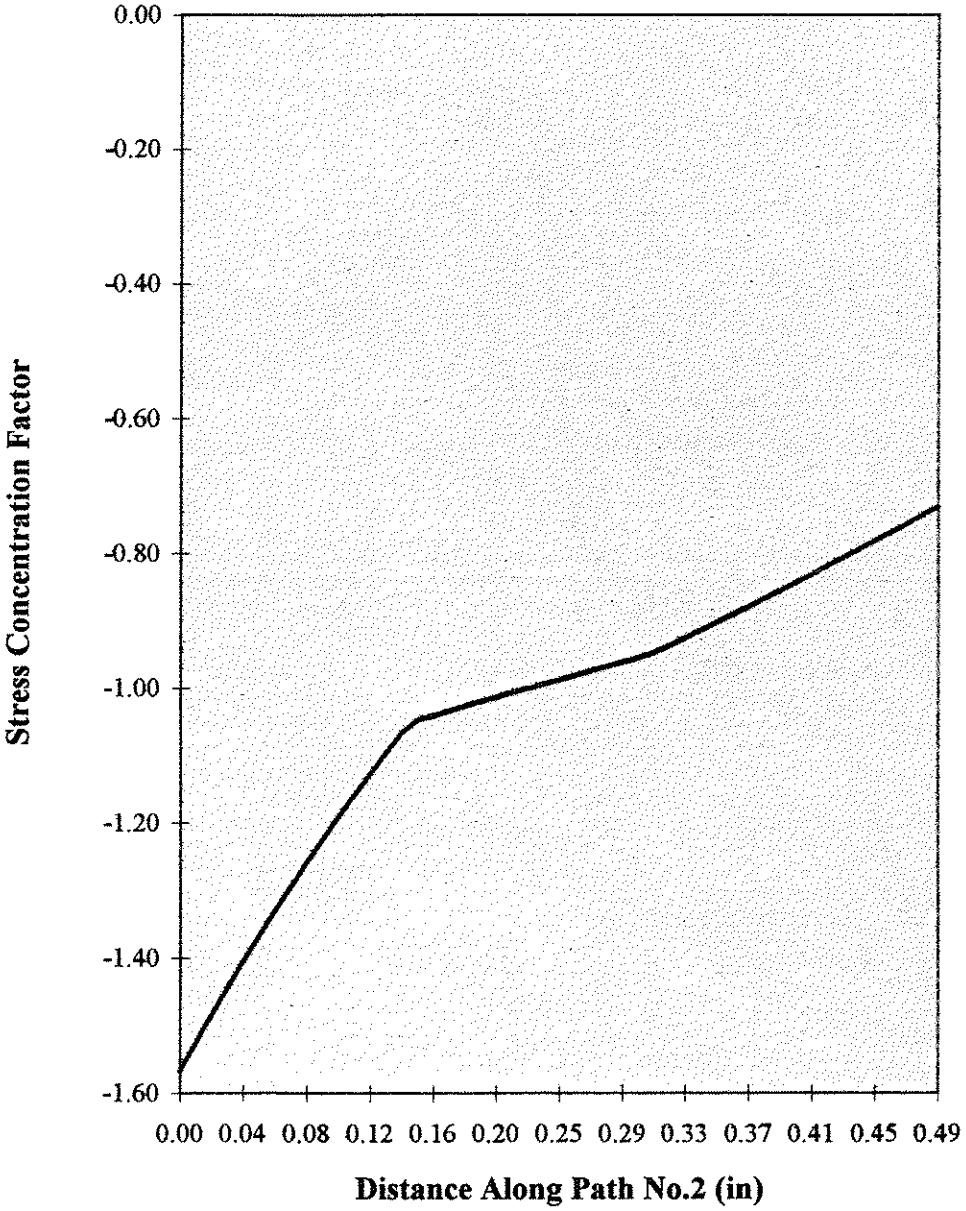

Fig. 3.3-3

Stress (SZ) vs. Distance Along Path No. 3 for Case112

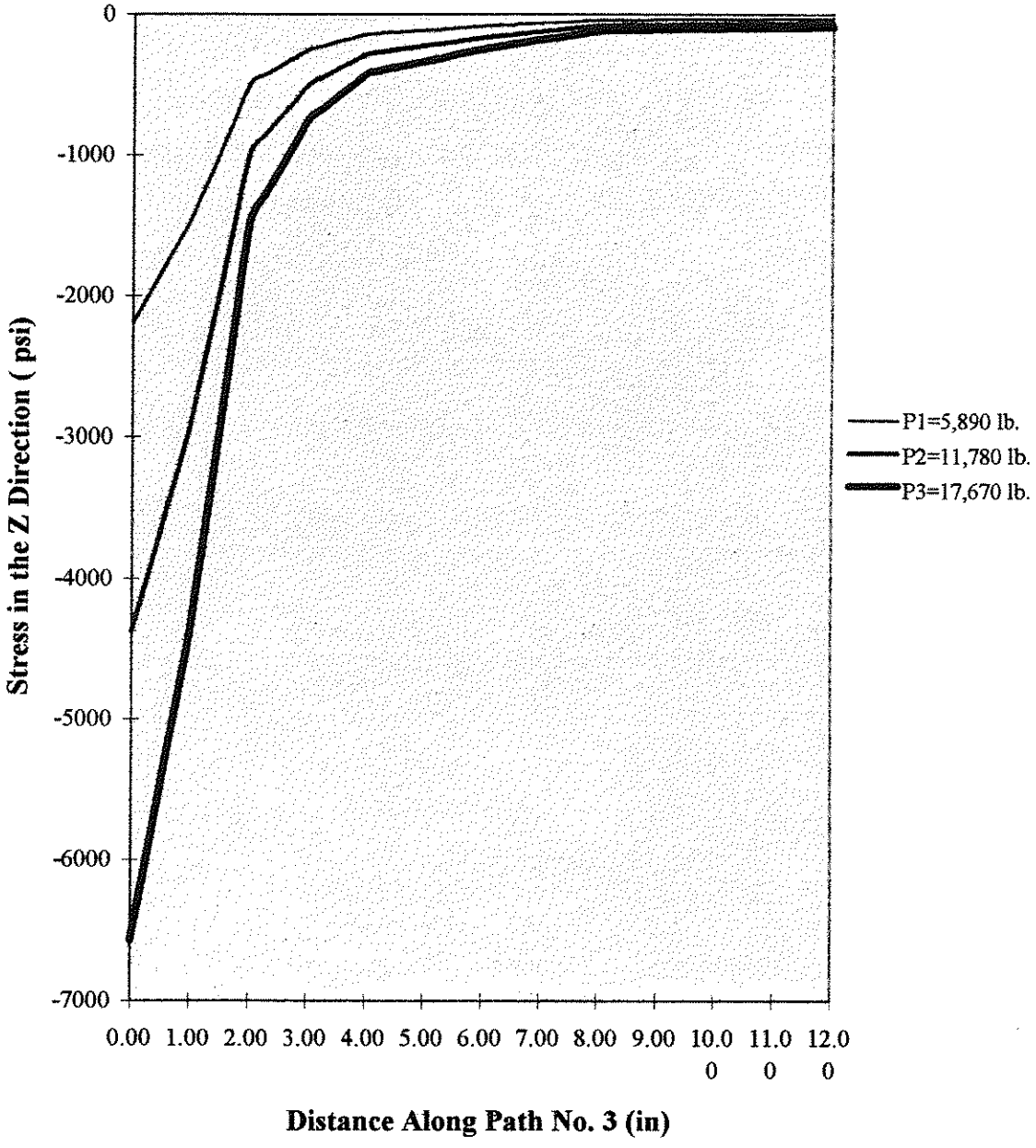

Fig. 3.3-4

example at a load level P2 in Case110, the maximum compressive stress is about -4800 psi, whereas it is reduced to about -4400 psi in Case112 or about a 10 % reduction.

Based on the comparison between the results from Case110 and Case112, the differences in stress distribution and stress concentration variation along Paths No.1, No.2 and No.3 are observed. Obviously, any differences are caused by the addition of concrete cover behind the head. So it could be assumed that concrete behind the head does contribute to concrete bearing capacity in terms of providing more resistance against head deformation and thus reducing the stress level and stress concentration factor on the concrete bearing area.

3.4 CASE122

The difference between Case112 and Case122 is the thickness of the head. In Case112 a 0.5 in head thickness is used while in Case122 the head thickness is increased to 0.75 in. (see "Input Parameters For Case122" in the following page.). This change is intended to form a basis of comparison between these two conditions in terms of head thickness influence on stress distribution in the head and concrete.

From the discussion in the previous models, it has been noted that in most cases the stress level in the concrete bearing area reaches a high value when the stress in the head is still low when compared to commonly used steel strengths. So the strength of the steel is not a concern if the ratio of head area to bar area is reasonable at about 5. The major concern is the concrete bearing capacity, which is mainly controlled by the bearing area. However, the change in head stiffness does effect the stress distribution in concrete bearing area. In Case112 the concrete cover behind head helps increase head bending stiffness. Also, it is known generally that the head behaves in two-way bending, especially in Case110. From this point of view, an increase in head thickness should increase the bending stiffness of head and thus distribute the compression force more evenly over the concrete in bearing under the head. This anticipated behavior is verified by the results from this model.

The curves displayed in Fig. 3.4-1 indicate that the stress distribution pattern along Path No.1 for the head in Case122 is similar to that in Case112. However, the overall stress level is reduced because of the increase in head thickness. At load level P2 condition as an example, the maximum compressive stress is about -12,500 psi , which is about 89% of the maximum compressive stress in Case112. The same situation is applicable to the average stress concentration factor along the Path No.1 in this model. So the variation of head thickness effects the stress variation in head, although change is not large at about 11%

The major input parameters for Case122 are listed below:

Input Parameters for CASE122

Item	Value	Remark
1. Finite Elements:		
concrete and steel	ANSYS solid 42	(4 node element)
concrete and steel	ANSYS solid 45	(8 node element)
2. Modules of Elasticity:		
steel	$E_s = 29.0 \times 10^6$ psi	
concrete	$E_c = 3.6 \times 10^6$ psi	
3. Poisson's ratio:		
steel	$\mu_s = 0.3$	
concrete	$\mu_c = 0.2$	
4. Geometry:		
bar diameter	$D_b = 1$ in	
bar area	$A_b = 0.785$ in ^{2}	
head thickness	$H_t = 0.75$ in	
Head area	$A_t = 3.925$ in ^{2}	$(At = 5 \times A_b)$
long edge of head	$H_y = 1.98$ in	$(H_y = \sqrt{At})$
short edge of head	$H_x = 0.99$ in	$(H_x = H_y/2)$
cover behind head	$H_c = 2$ in	
5. Loads:		
P1	5,890 lb.	$(P1 = 0.5 \times 15000 \times A_b)$
P2	11,780 lb.	$(P1 = 0.5 \times 30000 \times A_b)$
P3	17,670 lb.	$(P1 = 0.5 \times 45000 \times A_b)$

Stress (SZ) vs. Distance Along Path No. 1 for Case122

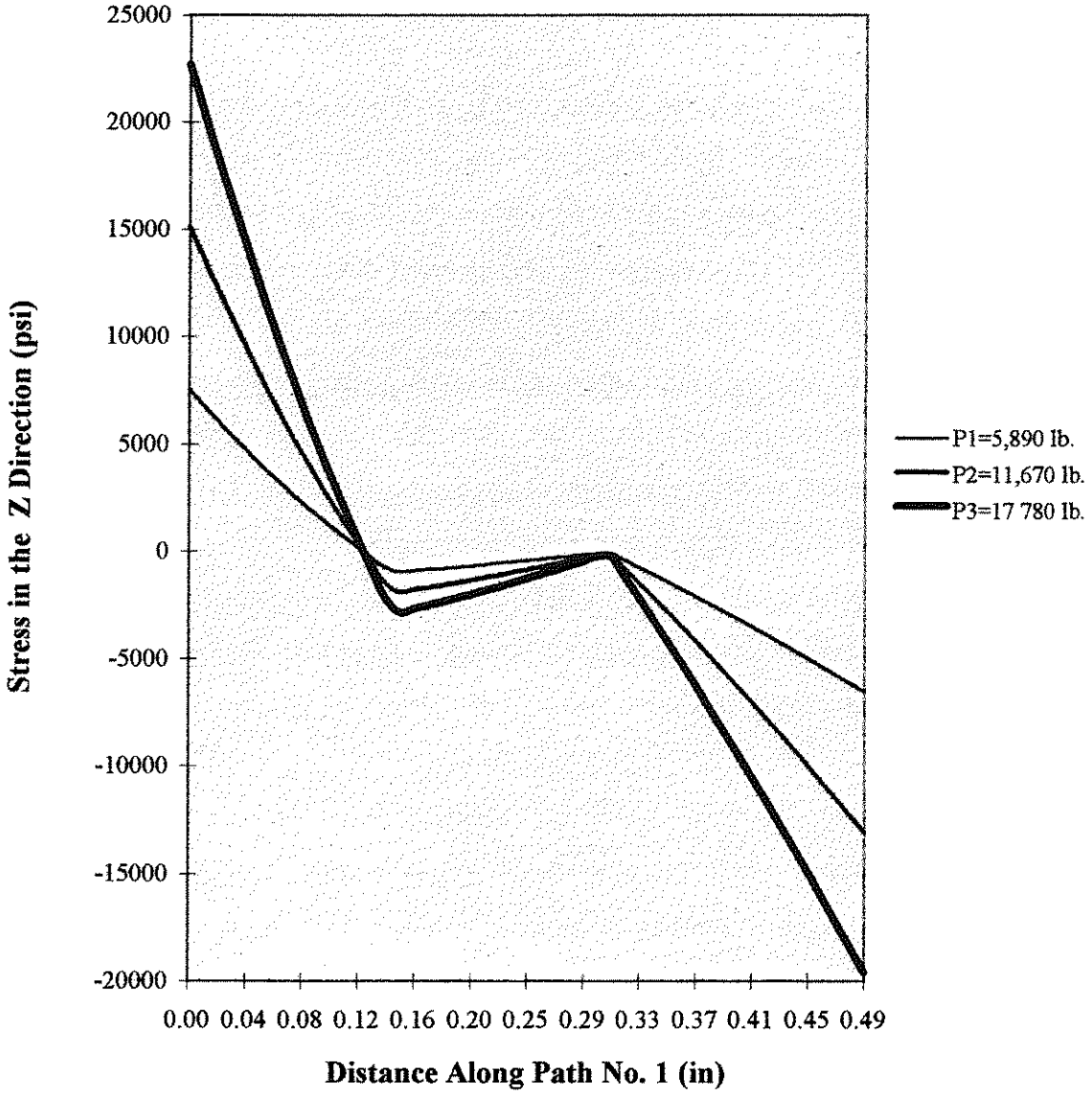

Fig. 3.4-1

Although there is no large change in stress distribution along Path No.1 as mentioned before, the stress variations along Path No.2 in Case122 are changed by increasing the head thickness. The overall stress concentration along the Path No.2 is reduced significantly because head stiffness is increased, so that the head is able to distribute the compression force over the concrete bearing area more evenly.

It is interesting to see the different stress distribution features along Path No.2 in this model as compared to that in Case112. From Fig. 3.4-2 if a path segment is selected that lies from the path starting point to a point that is about 0.49 in. away; in other words, the path segment is the segment that is under the head direct compression. For each load level condition, it can be seen in Fig. 3.4-2 that there are three "steps" in the stress distribution curve. The first step begins at the path starting point where the maximum compressive stress occurs and ends at the point about 0.15 in. away from the starting point. Within the first step the compressive stress decreases linearly along the path. The second step starts at the end of first step and stops at the point about 0.31 in. away from the starting point. The compressive stress basically has no obvious change within this second step and the curve is essentially a "plateau". After that, the third step begins and the compressive stress reduces again relatively slowly as compared to the first step.

By reviewing Fig. 3.3-2 it is noticed that there is no "plateau" along Path No.2 in Case112. In Case112 within the counterpart of the selected segment in Case122, the compressive stress distribution curve basically has only two "steps". The overall stress level along Path No.2 in Case112 is higher than that in this Case122. On the other hand, the average stress concentration factor in Case122 is lower than that in Case112. From Fig. 3.4-3 it is observed that the stress concentration factor varies from -0.68 to -1.21. It is only about 77 percent of that in Case112.

Stress (SZ) vs. Distance Along Path No. 2 for Case122

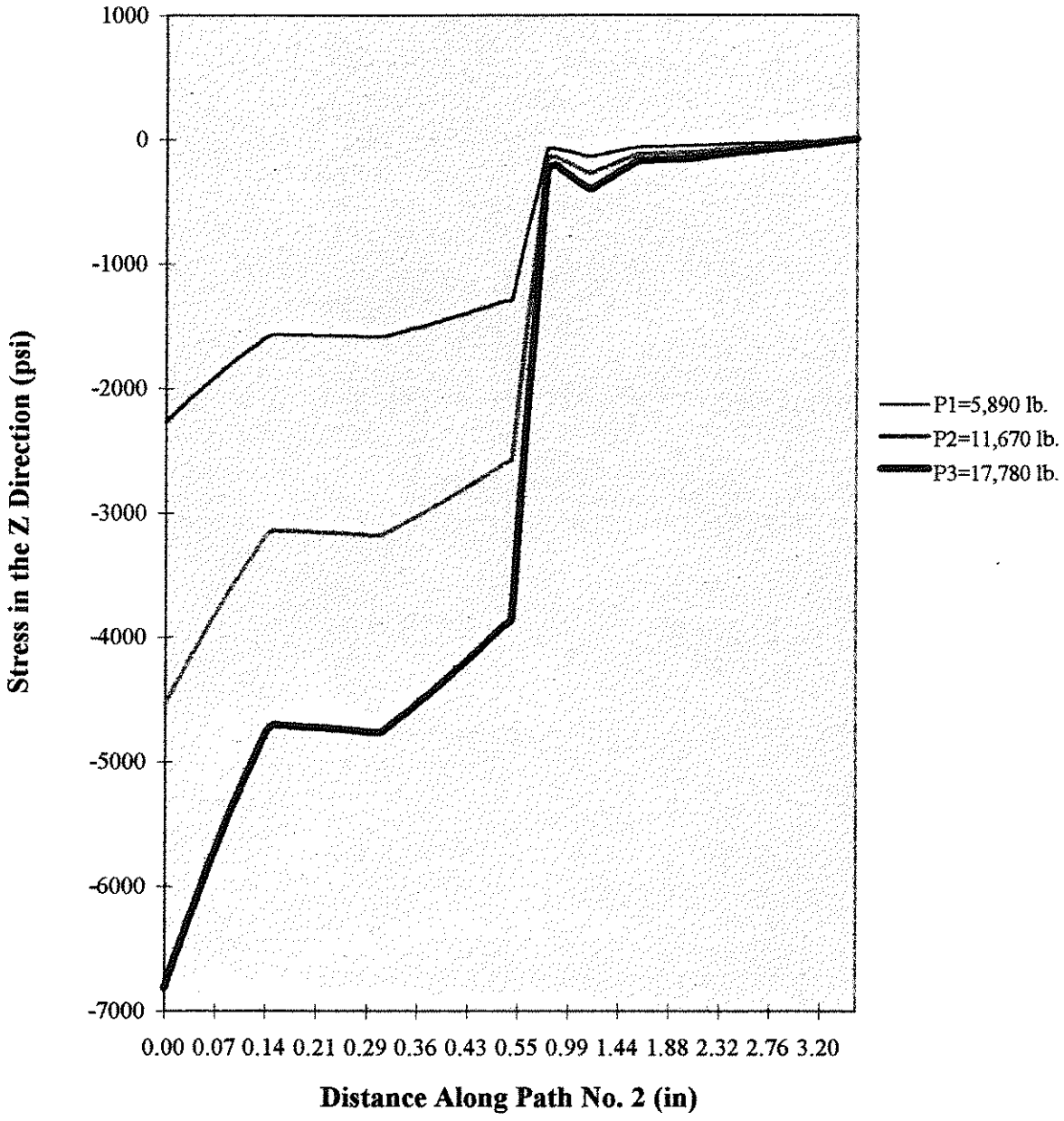

Fig. 3.4-2

Stress (SZ) Concentration Factor vs. Distance Along Partical Path No.2 for Case122

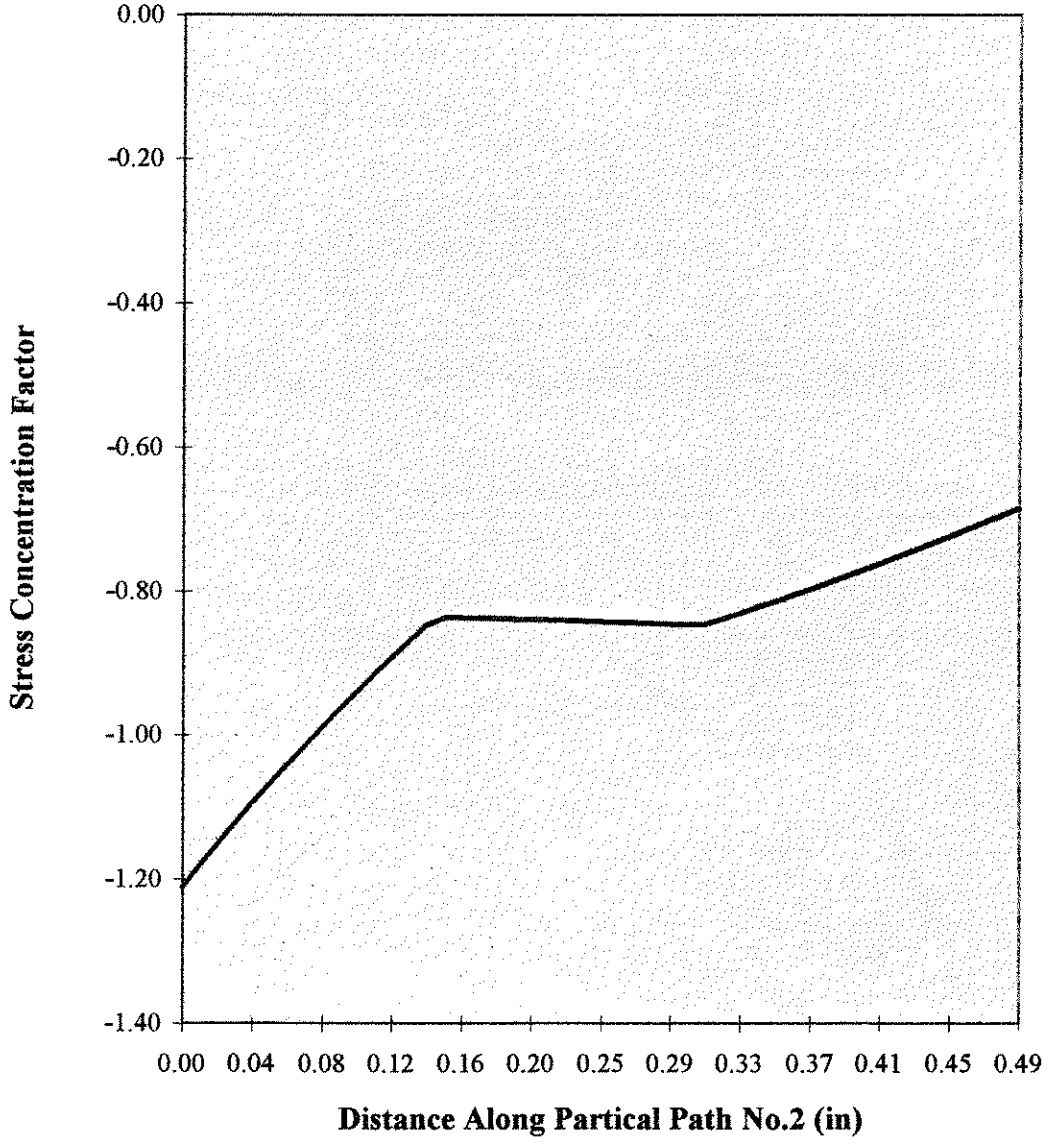

Fig. 3.4-3

Based on the comparison above it can be assumed that the "plateau" in the second step helps reduce the overall stress level and the stress concentration over the concrete bearing area along the Path No.2. This change is a benefit from head thickness increment. Moreover, the stress reduction in longitudinal direction, which is usually displayed on Path No.3, also is found but not presented in this section. In the longitudinal direction the stress reduction is mainly occurred within a distance of about 4 inches from the starting point of Path No.3. After that, the stress distribution behavior is basically same as the other models discussed before. Therefore, using a rigid head in terms of relatively high bending stiffness is helpful in headed reinforcement applications.

For these preliminary models, the discussion of head and concrete interactive behavior so far is based on Cases110, 112, and 122. These cases belong to the first group of preliminary models and have the same ratio of head area to bar area, that is, $A_t = 5\ A_b$. The comparisons made in the previous discussions focused on the influence of the different variables on the stress and strain distributions along the three selected paths within the models. These variables included the concrete cover behind the head and the head thickness. What follows is an extension of the variables examined to include head area.

3.5 CASE212

Case212 is one of models that belong to the second model group in which the ratio of head area to bar area is increased 7.5 to 1, that is, A_t =7.5 A_b. The differences of input data between Case122 and this Case212 are the head area and head thickness. In this model the head area is 1.5 times of head area in Case122 whereas the head thickness in Case122 is 1.5 times of head thickness in this model (The computer input parameters are listed in the next page). The purpose to compare this model to Case122 primarily in terms of effectiveness of materiel usage based on stress concentration factor concept is intended..

As expected, using a relative large head area A_t, or in other words a large effective contact area A_{te}, where $A_{te} = A_t - A_b$, the overall normal compressive stresses over head and concrete bearing area are decreased. However, from the point of view of stress concentration, an increased head area does not necessarily mean a reduction of the stress concentration level in some locations within concrete bearing area. In Case212 the head area increased but not the head thickness. This means that the so-called "effective" contact area is increased but the head bending stiffness, however, is decreased. As we know the bending stiffness effects the stress variation on the head itself and also influences the stress distribution over the concrete bearing area. From the results of both Case212 and previous Case122 the stress and strain distribution behavior along Path No.1 and Path No.3 are found to be basically the same. Due to the head area increase the average normal compressive stress along Path No.1 in Case212 is lower than that of in Case122 by about 14 %. However, the maximum stress concentration factor of about 3.60 is larger than that of 3.37 in Case122. This is because using an enlarged head area without increasing the head thickness causes a disproportional change in stresses. It is that the head bending stiffness is decreased so that the head becomes more flexible. The stress variation along Path No.3 in longitudinal direction in Case212 is reduced slightly as compared to the situation in Case122, though the head area is enlarged.

The major input parameters for Case212 are listed below:

Input Parameters for Case212

Item	Value	Remark
1. Finite Elements:		
concrete and steel	ANSYS solid 42	(4 node element)
concrete and steel	ANSYS solid 45	(8 node element)
2. Modules of Elasticity:		
steel	$E_s = 29.0 \times 10^6$ psi	
concrete	$E_c = 3.6 \times 10^6$ psi	
3. Poisson's ratio:		
steel	$\mu_s = 0.3$	
concrete	$\mu_c = 0.2$	
4. Geometry:		
bar diameter	$d_b = 1$ in	
bar area	$A_b = 0.785$ in^2	
head thickness	$H_t = 0.5$ in	
head area	$A_t = 5.89$ in^2	($A_t = 7.5 \times A_b$)
long edge of head	$H_y = 2.43$ in	($H_y = \sqrt{At}$)
short edge of head	$H_x = 1.22$ in	($H_x = H_y/2$)
cover behind head	$H_c = 2$ in	
5. Loads:		
P1	5,890 lb.	($P1 = 0.5 \times 15000 \times A_b$)
P2	11,780 lb.	($P1 = 0.5 \times 30000 \times A_b$)
P3	17,670 lb.	($P1 = 0.5 \times 45000 \times A_b$)

The comparison between Case212 and Case122 regarding stress distribution along Path No.2 is one of the major interests in the discussion of this section. Since these two models have different head areas and head thickness, several approaches from different perspectives are taken in discussing the results from these cases.

First, the general compressive stress distribution pattern in this Case212 is different from that in Case122. From Fig. 3.5-1 it can be seen that the stress variation curve for each load level in Case212 basically has two steps along the distance from the path starting point to the point that matches the edge of the head. Within the first step, which starts from the starting point of the path to the point about 0.12 in. away the stress level drops quickly as in the situation of Case122 shown in Fig. 3.4-2. The range of the second step is from the end point of the first step to a point 0.72 in. away. In the second step, the stress decreases relatively slowly compared to that in the first step. Generally, the change of slope in the stress distribution curve is smoother and it looks like a single curvature line compared to that in Case122. Review of Fig. 3.4-2, shows that there are basically three steps in the counterpart segment of stress distribution curve and a "plateau" appears within the second step. The curves appear to be double curvature lines. The "plateau" indicates in Case122 that the stress distributes more evenly over the concrete bearing area within the "plateau" range. However, this cannot be seen in Case212.

Second, the average compressive stress in Case212 is lower than that in Case122 , but the maximum compressive stress is greater than that in Case122. The results indicate that average compressive stress over the concrete bearing area is -2865 psi in Case212, whereas the average compressive stress in Case122 is -3254 psi. So the average compressive stress in Case212 is about 88% of that in Case122, which is a good result. The average stress reduction is expected due to the enlarged head area used. However, the maximum compressive stress, in load level P2 for example, is about 5300 psi which is greater than that of 4600 psi in Case122. That is, the maximum compressive stress in Case212 is increased about 15% over that in Case122, even an enlarged head area was

Stress (SZ) vs. Distance Along Path No. 2 for Case212

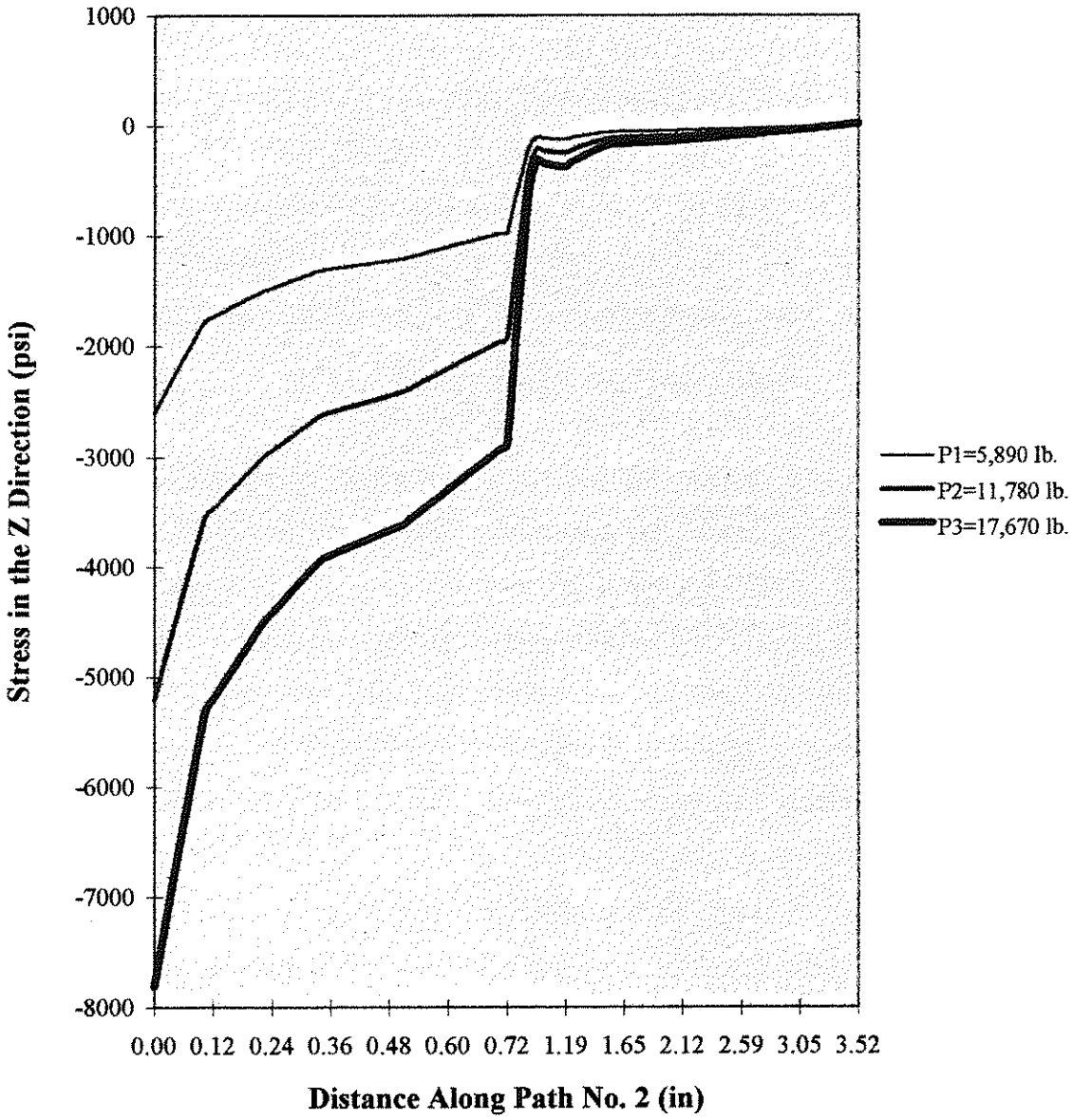

Fig. 3.5-1

used. This result implies that a relatively lower average stress level over the concrete bearing area does not mean that the stress intensity is lower in all locations within the bearing area. If structure is sensitive to stress concentration, counting on a relative lower average stress level might not be reliable for structural design.

Third, the compressive stress concentration factor in this Case212 is higher than that in Case122 because the head used in Case212 is more flexible than that used in Case122. Comparison between this Cases212 and 122 regarding stress concentration factor variation along Path No.2 shows that in Case212 the compressive stress concentration factor varies from -0.83 to -2.26, while the factor in Case122 falls within the range of -0.68 to -1.21. This result confirms again that in the condition of a lower average stress over the concrete bearing area may still produce a higher stress concentration within that area.

In any normal structural application, a high stress concentration situation generally is unwanted or should be reduced as much as a designer can do. From this point of view, a good design rule for the head size is a complicated parameter to determine. It depends on many variables involved in the head-concrete interaction. If concrete compressive strength and bar area are given, selecting a reasonable head size, including area and thickness, is basically based on the consideration of having a reasonable balance between average stress level over the bearing area and controlling the stress concentration within the bearing area.

In general the larger the head area, the "lower" the average stress level; the thicker the head, the stiffer the head. However, the head size must be limited by practical application in which the size and the cost of the head should be reasonable. Thus, using a reasonable ratio of head thickness to edge length of head, should be considered in application of head reinforcement. Comparing Case212 to Case122, for example, the head thickness and head area are different from each other but the steel volume used are same in both cases. That is in Case212, head area is 7.5 times of bar area (A_t =7.5 A_b) and head thickness is 0.5 in. The volume of steel in the head used is equal to 0.5 x 7.5 A_b = 3.75 A_b.

In Case122, the head is 5 times of the bar area ($A_t = 5\ A_b$) and the head thickness is 0.75 in. The steel volume used is equal to $0.75 \times 5\ A_b = 3.75\ A_b$. So in both models the steel volumes are the same. However, the stress distribution status along Path No.2 is different in each case. The differences in average stress and stress concentration have been discussed before and suggest that using a relatively thicker head is better in achieving lower stress concentration over concrete bearing area for a given steel volume. The average stress level follows approximately the same general rule.

3.6 Summary of Preliminary Models

So far in the limited Finite Element analysis conducted for the selected preliminary models, the results have been discussed. Through the results of obtained from the Finite Element models from Cases110, 112, 122 and 212, the fundamental understanding about the interactive behaviors of head and concrete are obtained. The comparisons among the results from the different model cases have yielded some interesting information that is useful for the further study of headed reinforcement applications. The analysis of the information has been the emphasis with the focus on concept interpretation rather than on numeral manipulation. As a summary of the analysis of the preliminary models, several points need to be recalled from the comparisons and discussions among the many models:

1. When headed reinforcement is embedded in a concrete volume, the head and concrete interactive behavior is similar to that of a spread footing under a column buried in hard soil. The differences in this analogy are in loading direction and the different materials.

2. The structural behavior of the head is basically like a stiff plate in two-way bending. The strength design method for head might be similar to a base plate or a footing, conceptually. The head bending stiffness is important because it effects the stress distribution on itself and the stress concentration level over the concrete bearing area. According to experiment and analysis, the stress level on head is lower than the yielding point of reinforcing steel. So the concrete bearing capacity is a major concern and efforts to reduce stress and stress concentration levels over the concrete bearing area should be taken by the designer. Thus, in practice head stiffness may control the design for head. Based on analysis and judgment, a ratio of head thickness to the head length, measured from the edge of the bar to the edge of the head, $0.6 \sim 0.8$, is recommended if the stress concentration factor is to be controlled in the range of 1.55 to 1.5 within concrete bearing face.

3. Concrete bearing capacity plays an important role in headed reinforcement application. The mode of specimen failure could be a shear failure in the concrete under the head edge, or a concrete bearing capacity failure directly under the head, or a combination of these two. Under same loading condition, the compressive stress concentration factors in the concrete bearing face vary depending on the head size and its bending stiffness, as well as the presence of concrete cover behind the head. The maximum stress concentration factors are 1.86, 1.57, 1.21 in models Cases110, 112, 122, respectively, and 2.26 in Case212. The results indicate that using a stiffer head is recommended because controlling the stress concentration level is important, as controlling the average stress in practice. If head steel volume is given, using a thicker head is effective in controlling stress distribution and also saving steel.

4. Based on the observation of stress distribution in both the lateral and longitudinal directions through Paths No.2 and No.3, it is recommended that crossing reinforcement at the front of the head be provided to carry the shear around the edge of head. Also, it is recommended that similar sets of reinforcement at 2 or 3 in. spacing from the head face to about 4 or 6 in. away in the longitudinal direction. These bars are to provide shear capacity for the concrete around the head and reinforce the concrete bearing capacity. Similar recommendations were made by Wright and McCabe in their experimental study.

CHAPTER 4

Advanced 3D Linear Model

A more advanced model was created in the hope of improving the model's performance. A relatively advanced 3D linear model was constructed and results are presented in this chapter.

In previous section several preliminary finite element models have been presented. The results from the preliminary models provided useful information about general headed bar and concrete behavior. However, the discussion was based on the results which were selected from the three typical paths within those models, so the whole "picture" was not presented. Also, in the previous models at the interface of head and concrete elements , the head and concrete sheared the same nodes.

This situation could have caused at least two unwanted behaviors during the analysis: 1) relative lateral movements between the head and the concrete bearing face were, so use of different Poisson's ratios at the interface really did not matter; 2) relative longitudinal movements between interface of the head and the concrete bearing face also were restrained so it did not conceptually present the compression only relationship at the interface of steel and concrete. Therefore, the changes made in this advanced 3D linear model were: 1) compression only boundary condition at the interface of the head and the concrete bearing face was created; 2) more visual plots through color prints are provided for discussion of results; 3) also, the concrete block volume was reduced and the bar shortened in order to save computer resources.

4.1 Introduction to Modeling

In order to use similar variables that were used in the experimental work, the head area used in this model is taken as about ten times that of the bar area, and the head thickness is 0.60 in., in experimental work the head area is 4900 mm ^{2} and the head thickness was 15 mm).

Finite Elements were selected from the ANSYS5.3 element library and included solid-42 with 4 nodes, solid-45 with 8 nodes, and link-10 with 2 nodes. As in the preliminary models element 42 is mainly used as an assistance to building the 3D solid model with solid 45 elements during modeling procedure, and element 42 was usually "unselected" before a solution was executed. The newly employed element link 10 was used to create compression only boundary condition at the interface of the head and concrete. This compression only condition was used in both front and back faces of the head.

The materials used in the model are still treated as linear. For concrete, a Poisson's ratio of 0.2 and a Modules of Elasticity of 3.6×10^6 psi are used, based on the assumption of a 4000 psi compression strength. For steel, a Poisson's ratio of 0.3 and a Modules of Elasticity of 29.0×10^6 psi are assumed as before.

According to the experimental work, the maximum applied load that a typical specimen could hold is about 36 kips. In order to save time there is only one load level used in the analysis of this model corresponding to one-half of the maximum because one-half model was used. The applied load is equal to the load level P3 used in preliminary model cases, which is 17,670 lb. In the other words, this is equivalent to a nominal tension stress of 45000 psi on the bar cross sectional area, as defined in preliminary cases. However the load is applied on the two nodes at the tip of the bar by using two concentrated loads. The input parameters for this model are listed in next page for reference.

Input Parameters for Advanced Linear Model

Item	Value	Remark
1. Finite Elements:		
concrete and steel	ANSYS solid 42	(4 node element)
concrete and steel	ANSYS solid 45	(8 node element)
concrete and steel links	ANSYS link 10	(2 node element)
2. Modules of Elasticity:		
steel	$E_s = 29.0 \times 10^6$ psi	
concrete	$E_c = 3.6 \times 10^6$ psi	
3. Poisson's ratio:		
steel	$\mu_s = 0.3$	
concrete	$\mu_c = 0.2$	
4. Geometry:		
bar diameter	$d_b = 1$ in	
bar area	$A_b = 0.785$ in ^{2}	
head thickness	$H_t = 0.59$ in	
head area	$A_t = 7.595$ in ^{2}	($A_t \cong 10 \times A_b$)
long edge of head	$H_y = 2.756$ in	($H_y = \sqrt{At}$)
short edge of head	$H_x = 1.378$ in	($H_x = Hy/2$)
cover behind head	$H_c = 2$ in	
5. Load:		
P	17,670 lb.	($P = 0.5 \times 45000 \times A_b$)

The basic procedure used in modeling here is similar to that in preliminary models. However, the most difficult part of modeling in this case is creating the compression only boundary condition at the interface of the head and concrete bearing areas. This is achieved by using link 10 elements as compression only elements. In doing so, at the front and back faces of the head gaps were created between the head and concrete during modeling. That is, the elements of the head and concrete were separated. These elements shared common nodes in preliminary models. Now they were spaced apart by a distance of 0.005 in. and within this distance the link 10 elements were placed. The link 10 elements require the definition of a real physical distance for the links. The related nodes of elements from both the head and concrete sides were connected by using link 10 elements which are defined as rigid in compression but flexible in tension. So, based on these assumptions, the relative lateral movements between the head and concrete should be allowed in the model. In the longitudinal direction there is no tension action but there is a compression force between the interface of the head and concrete. To conceptually show the model size, loading direction, and boundary conditions, including the special features around the head area, Fig. 4.1-1 is provided.

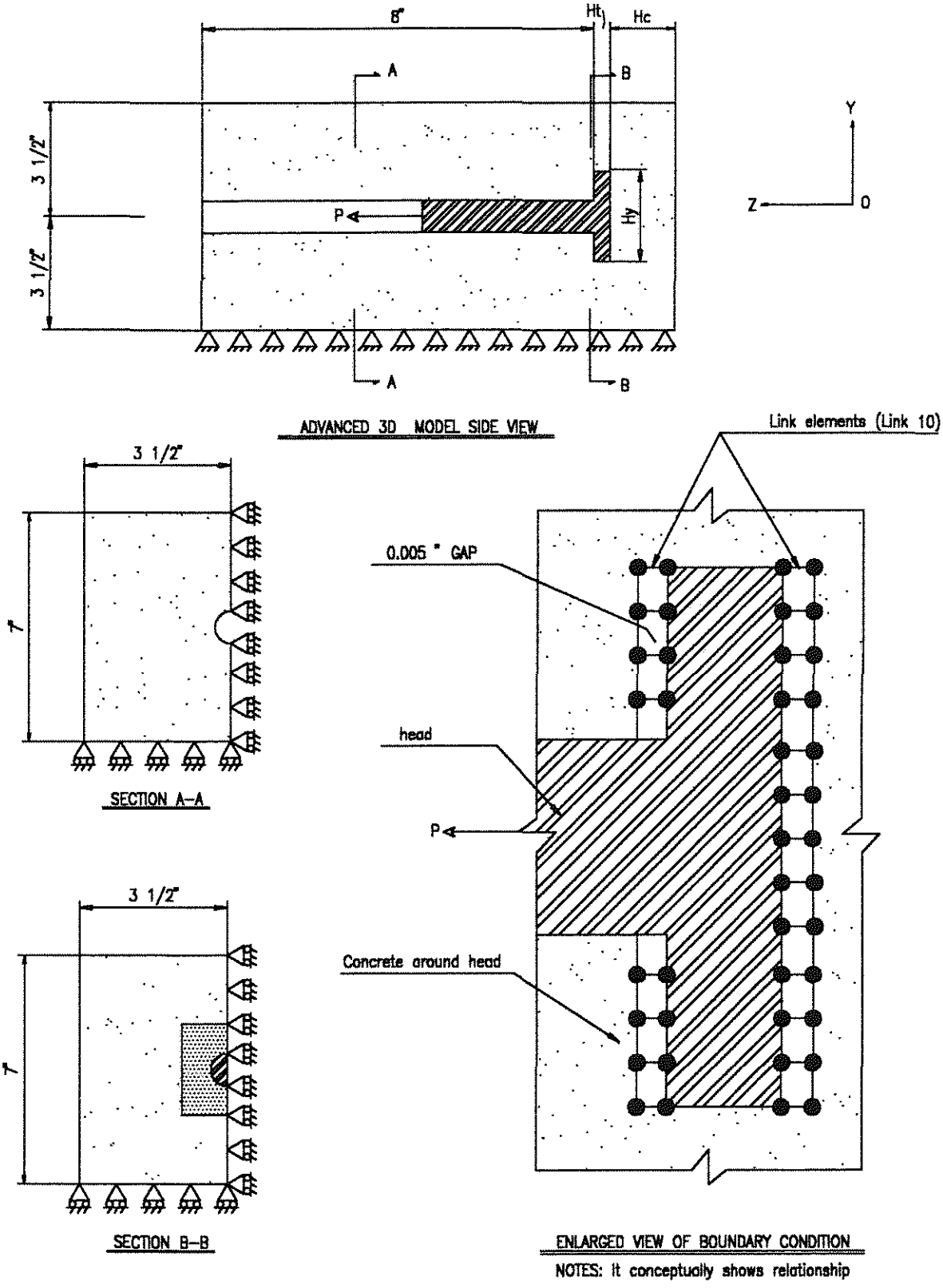
8"
Ht
Hc
A
B
3 1/2"
3 1/2"
P
Hy
Y
Z
O
A
B
ADVANCED 3D MODEL SIDE VIEW
3 1/2"
7"
SECTION A-A
3 1/2"
7"
SECTION B-B
Link elements (Link 10)
0.005 " GAP
head
P
Concrete around head
ENLARGED VIEW OF BOUNDARY CONDITION
NOTES: It conceptually shows relationship

Fig. 4.1-1

4.2 Discussion of Results

Instead of using plots that are taken from the three typical paths which were pr-selected in the preliminary models, color plots are employed for presentation of the ANSYS results in this model. This presentation is intended to show the entire stress distribution over the head and concrete in the 3D situation so as to give a complete visual impression.

Before the results can be discussed, one further explanation about the loading has to be made. As mentioned before, the loads in this model were applied as two concentration loads at two nodes at the tip of the bar, this caused very localized high stress concentration at the end of the bar and affected a distance in the region of the bar. Consequently, the colored stress legends on the prints in Fig. 4.2-1 indicate an extremely high stress level on the plots due to the linear material assumption used. The head shown in Fig. 4.2-1 with principal (S1) stress contours on it, is removed from the entire model pictorially by using selection feature in ANSYS. From the oblique view of principal stress contour on the head in Fig. 4.2-1, the entire stress distribution over the head can be seen. The principal stress over the major part of the head is between -3399 psi and 56,117 psi. If it is assumed that an average stress level is about 26,000 psi and the maximum is about 56,000 psi, this indicates again that the overall stress on the head is below the yield point of 60,000 psi. So, the strength of steel again is not a concern as in the preliminary models. Compared to the maximum principal stress S1 caused by load level P3 in Case110, shown in Fig. 3.2-4, which is about 38,000 psi, the principal stress in this model is much higher than that in Case110 though same load is applied in both cases. This result could be due to the fact that the head area is larger but the head thickness is only slightly increased in this model. Thus, the stress from bending moment, which is major component of principal stress S1, has been increased. From the deformed shape of head in the picture, head is shown to be deformed in a manner similar to a two-way cantilever plate as discussed in preliminary cases. Also, there is no resistance offered by tension between the steel and concrete.

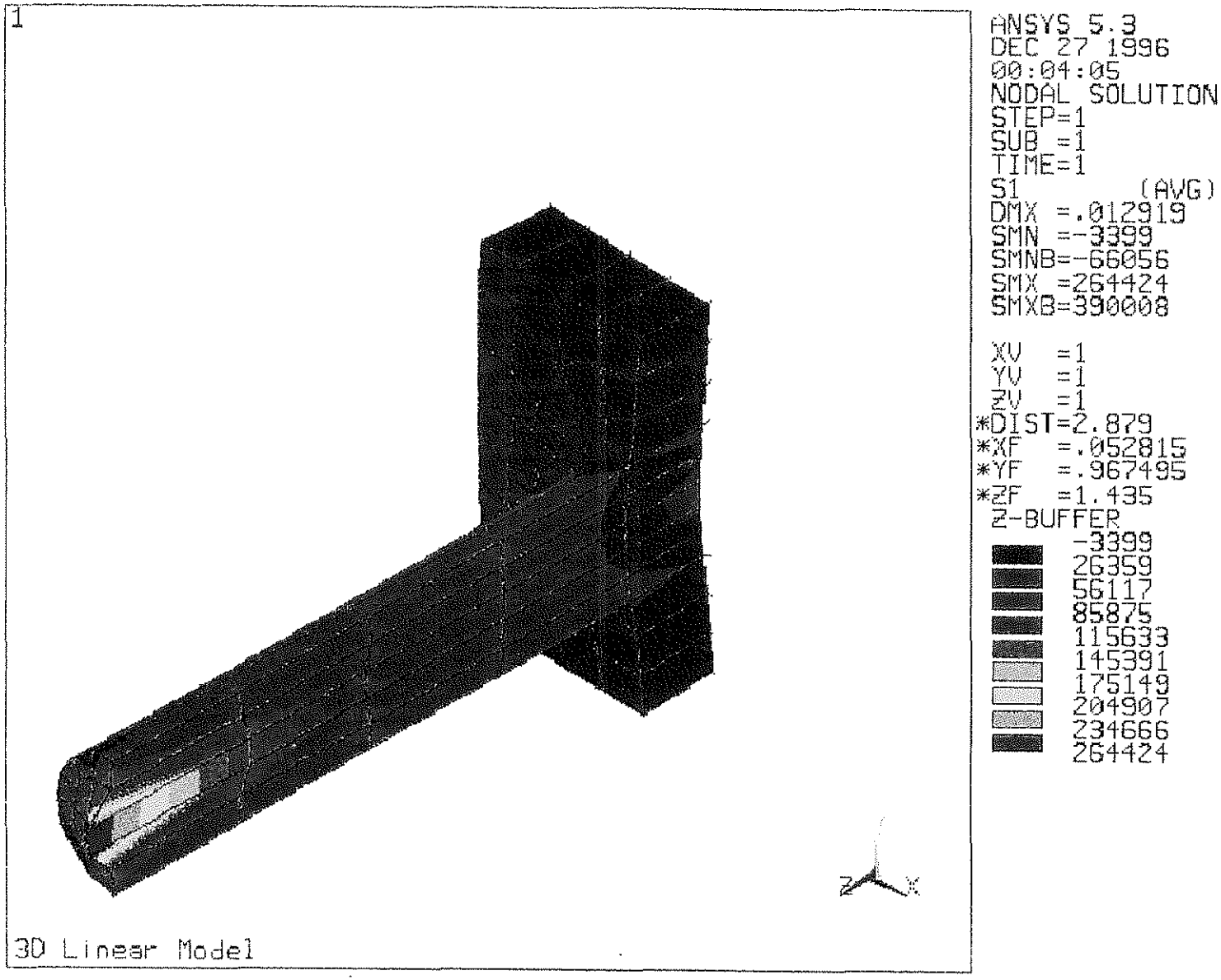
1
ANSYS 5.3
DEC 27 1996
00:04:05
NODAL SOLUTION
STEP=1
SUB =1
TIME=1
S1 (AVG)
DMX =.012919
SMN =-3399
SMNB=-66056
SMX =264424
SMXB=390008
XV =1
YV =1
ZV =1
*DIST=2.879
*XF =.052815
*YF =.967495
*ZF =1.435
Z-BUFFER
-3399
26359
56117
85875
115633
145391
175149
204907
234666
264424
Z
X
3D Linear Model

Fig. 4.2-1

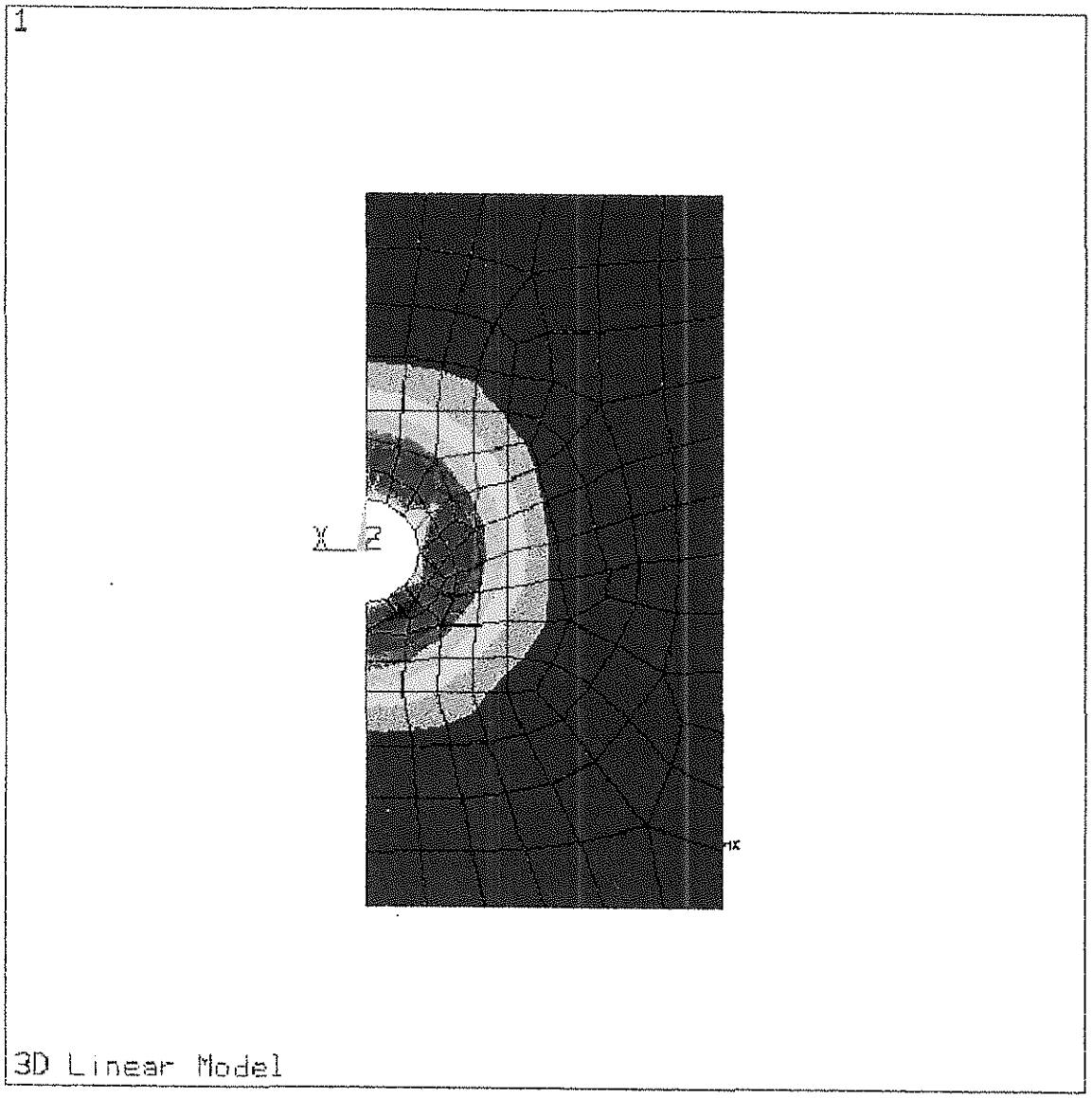
1
ANSYS 5.3
DEC 26 1996
23:42:03
NODAL SOLUTION
STEP=1
SUB =1
TIME=1
SZ (AVG)
RSYS=0
DMX =.012919
SMN =-4595
SMNB=-6507
SMX =34.304
SMXB=945.681
ZV =-1
*DIST=5.292
XF =-1.754
YF =.007192
ZF =4.227
Z-BUFFER
-4595
-4081
-3566
-3052
-2538
-2023
-1509
-994.49
-480.093
34.304
3D Linear Model

Fig. 4.2-2

The compressive stress variation over the concrete bearing area is shown in Fig. 4.2-2. This plot was created during the post processing stage of the ANSYS results by using series selection operation. The view shown is toward the positive Z (along the bar) direction over concrete bearing face in the X-Y plane.

The compressive stress distribution pattern over the concrete bearing face looks like a half "target" since half of the model was used. On the target several color rings are seen around the center of the target indicating the stress level changes from high to low at very inner ring to outer rings, sequentially. The stress ranges between about -4300 psi to -500 psi. There are a few higher stresses shown and these are more the effect of modeling than real behavior. From this information, it can be seen that the maximum compressive stress in this model agrees well with assumed concrete compressive strength of 4000 psi. Although this can not be considered as the typical case since only a limited number of Finite Element model have been analyzed, it does provide useful information for determining the ratio of head area to bar area in further research and application. The head area is 10 times the bar area and matches the head to bar area ratio which has been used in experiment work conducted at Kansas by Wright and McCabe. It also matches the requirements in the new ASTM standard A970-97 for welded headed bar.

In addition, the head thickness used in this model is 0.60 in. with a size of 2.756 in square. These sizes match the geometry used in tests. The ratio of head thickness to the head length is about 2.2 to 10. This is close to the values revealed in preliminary models where the ratio is within 2.5 to 10 and 3.8 to 10 though a higher ratio of 4 to 10 is recommended. Therefore, the head thickness used in the experiment is reasonable in terms of reducing stress concentration over the concrete bearing face.

Based on the assumption of using a nominal compressive stress defined as P/A_{te} = 2595 psi over the so-called ideal contact interface, the maximum compressive stress concentration factor is about 1.65. This value also is close to the average values indicated in the preliminary model cases. Hence, it could be a reasonable reference value for

compressive stress concentration factor over the concrete bearing area in application of headed bar reinforcement if relatively stiff heads are used and the ratio of head area to bar area is reasonable at 7.5 to 1.0. From the compressive stress contour plots shown in Fig. 4.2-1 and 4.2-2, it can be seen that the stressed area does not resemble a square area of the head, but rather a circular area. This result implies that using a ring area, like that shown in the plot, as an effective concrete bearing area with the appropriate stress concentration factor involved, could be useful approach during development of design formulas for headed bar application.

To observe the compressive stress variation in the longitudinal direction, Fig. 4.2-3 is employed. This oblique view shows the major part of concrete specimen isolated from the whole head-concrete model. The stress distribution contour on the plot displays not only the stress distribution in the longitudinal direction, but also in the lateral direction as well.

From the plot shown in Fig. 4.2-2, the stress distribution pattern on the bearing surface appears as several colored rings in plan view. Through the oblique view shown in Fig. 4.2-3, the stress distribution contours become 3D objects. Generally, they are several shell-like 3D objects with different features. The formation of each of theses seems to be an "extruded" shell in the Z direction. The higher the stress level, the shorter the "extruded" length from bearing surface; the lower the stress level, the thicker the shell becomes. Also, those shell representing higher stresses have no closed ends while the shells displaying relative lower stress have closed ends which look more like several "bowls" overlapping together. Like the stress variation in the lateral direction in the concrete bearing area, the stresses in the longitudinal direction vary from approximately -4300 psi to -500 psi. As expected, the higher stresses occur at those "open shells" around concrete, immediately under the head. In the longitudinal direction, the compressive stress influence reaches a depth of about 3.5 to 4 in. from the bearing surface and the stress reduces to a level of about -500 psi. The critical region lies within the distance from the bearing surface to a parallel section about one inch away from the bearing face. This

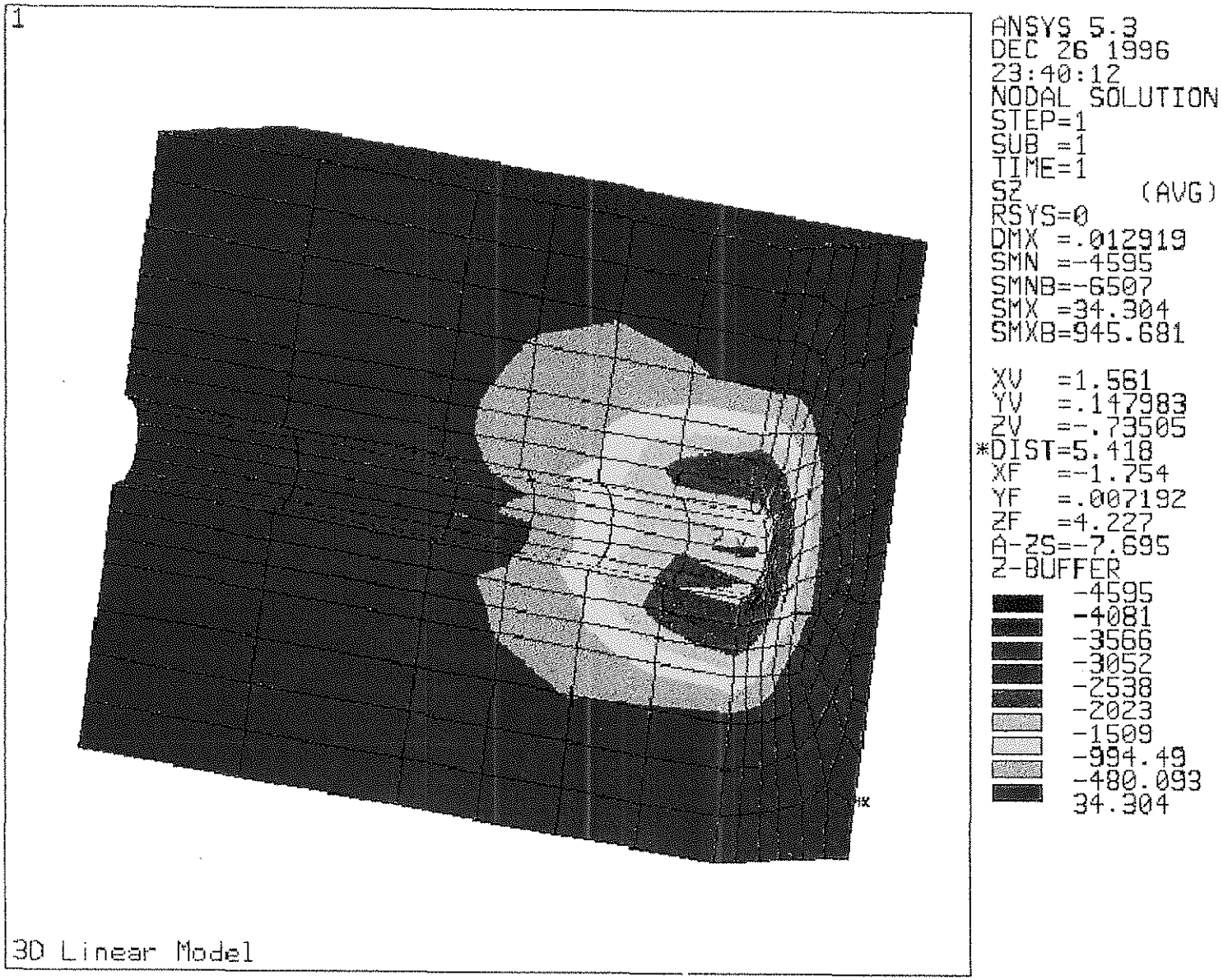
1
ANSYS 5.3
DEC 26 1996
23:40:12
NODAL SOLUTION
STEP=1
SUB =1
TIME=1
SZ (AVG)
RSYS=0
DMX =.012919
SMN =-4595
SMNB=-6507
SMX =34.304
SMXB=945.681
XV =1.561
YV =.147983
ZV =-.73505
*DIST=5.418
XF =-1.754
YF =.007192
ZF =4.227
A-ZS=-7.695
Z-BUFFER
-4595
-4081
-3566
-3052
-2538
-2023
-1509
-994.49
-480.093
34.304
3D Linear Model

Fig. 4.2-3

position is indicated in the plot that as section that intersects all the "shells" at that location.

By looking at the surface on which the longitudinal stress contours or fields are displayed, it can be seen that the upper field of the stress distribution is larger than that of the lower field in both the lateral and longitudinal directions. This behavior implies that the upper part of the model is under higher stress demands than that of the lower part of model. In other words, the upper part would reach a failure condition before the lower part. This behavior situation has been seen in the testing of specimens where cracking appeared at the top surface of the specimen first (Wright and McCabe). The explanation for this situation is: 1) Since restraints are applied on the bottom surface of model but not the top surface, the boundary condition is not symmetrical, though the model is. Therefore, the lower part of model has more restraint from the supports while the top surface is free from restraint on that face. For the lower part there is more confinement around the region and it provides both lateral and longitudinal support to the relatively highly stressed concrete within the region. This confinement causes triaxial compression stresses that increase the strength of the concrete. In other words, the triaxial compression situation helps to share the stresses, thus compressive stress in the Z direction (SZ) could be reduced under a given load. Whereas, the upper part has less restraint or confinement, compared to the lower part.

2) Because of the limitation of modeling, a bending moment (Mx) exists in the lower part of model due to the moment arm between the loading and the bottom surface of model; while there is no moment in the upper part which is above the loading direction, conceptually. This moment causes bending stress in the lower part of model so that it would balance certain compressive stress (SZ) though slightly. However, these limitations in modeling are not significant. The fact remains that failures observed in the laboratory were generally seen to initiate in the upper portion of the specimen, as predicted by 3D model. Thus, the correspondence between the 3D model and the test experience is satisfactory.

4.3 Summary of Advanced 3D Model

From the point of view of reflecting head and concrete interactive behavior, this 3D advanced Finite Element model conceptually has revealed similar results to those from the preliminary models. However, this model provides improved information than that of preliminary models because several aspects of the model have been improved. The compression-only boundary condition between the head and concrete is closer to the real interactive behavior of the head and concrete, which means a no tension state between the interface of the steel and concrete. Also, the boundary condition allows for the relative movement in both lateral and longitudinal directions so that the different material properties like Poisson's ratio and Modules of Elasticity can be truly meaningful in the Finite Element model. Moreover, the head size matches that of used in experimental specimens so that the results can be more informative compared to the test results.

Given the modeling and loading conditions in this case, the analysis results indicate that the maximum principal stress (S1) over head is still under the yield point of 60,000 psi, so the head strength is adequate. The maximum compressive stress over concrete bearing face, as well as in the concrete volume, is about 4300 psi which is slightly over assumed concrete compressive strength of 4000 psi. Due to high compressive stresses in this type of structure, the loss of concrete bearing capacity would be expected to be a typical failure mode, though the real stress status would be more complicated. The compressive stress concentration factor over the bearing face in this model is about 1.65, based on a reference nominal stress level of 2595 psi. High level stress concentrations will cause localized concrete crushing and cracking, so attention should be given to the stress concentration when considering headed reinforcing bar application. This observation means the head bending stiffness plays an important role in reducing the stress concentration factor under a given loading, and the head to bar area ratio is important because the head acts as a cantilever plate in two-way bending.

CHAPTER 5

Linear Model vs. Nonlinear Model

If the compressive stress and strain levels in concrete are relatively low compared to the concrete compressive strength and maximum strain allowed, the concrete behavior can be considered to be linear. As in the case of headed bar models, the compression force from the head not only causes higher stresses and stress concentrations over the bearing face, but also complicates the stress situation in adjacent regions, so localized concrete cracking and crushing can be expected. This behavior can be predicted by the linear cases through the high stresses displayed in the results in certain locations. However, the linear models do not permit evaluation of how high the stress will be in nonlinear behavior, and no evaluation of the redistribution of stress under nonlinear behavior has been observed. Therefore, the idea of creating a nonlinear model, and conducting a comparison between the linear and nonlinear models is introduced in this section.

A "2D" slice nonlinear model has been used to evaluate the nonlinear behavior. The so-called "2D" slice is in reality a 3D solid nonlinear model with solid nonlinear finite elements The reason for using "2D" slice model is to save time and computer resources. The model is called a "slice " because the thickness of the model is thin and it looks like 2D object cut from a 3D solid. The "2D" linear slice model having same model conditions as the "2D" nonlinear slice is compared.

5.1 Introduction to Modeling

Two names are used to refer to the two slice models. For the linear model Slice 1 is used, while the nonlinear model is called as Slice 2. The procedure of modeling both linear and nonlinear slice models are same except nonlinear elements used in Slice 2.

For both models, Finite Elements selected from the ANSYS5.3 element library are solid-42 with 4 nodes, solid-45 with 8 nodes, and link-10 with 2 nodes. The solid-65 with 8 nodes, which is concrete element with nonlinear behavior, is selected for Slice 2 only. Element 42 is mainly used as an assistance to building solid models during the modeling procedure as mentioned in previous cases. In Slice 1 element 45 is used for both steel and concrete while in the nonlinear Slice 2 model element 45 is used for steel only and element 65 is assigned to the concrete. As in the 3D linear advanced model, element link 10 is used to create a compression-only boundary condition at the interface of the head and concrete. The method of producing such type boundary is same as that used before. A generic model shown in Fig. 5.1-1 conceptually represents both the Slice 1 and Slice 2 models in terms of model sizes, boundary conditions, and loading directions. Note that the layout of the model is in the X-Y plane and loading is in negative X direction of global coordinate system. Since the models are "cut out" from a 3D solid and in order to create a stable "specimen", the restraints in the Z direction are applied to the both front and back cutting faces of slices. Thus, this type of boundary condition produces plane strain situation in the slice models, especially in the lower part of the models.

In both slice models many material properties are identical. For concrete, a Poisson's ratio of 0.2 and a Modules of Elasticity of 3.8×10^6 psi are used, based on the assumption of a 4500 psi compression strength; for steel, a Poisson's ratio of 0.3 and a Modules of Elasticity of 29.0×10^6 psi are assumed. However, for the nonlinear model Slice 2 there are several variables have to be provided for the solid element 65 so that the

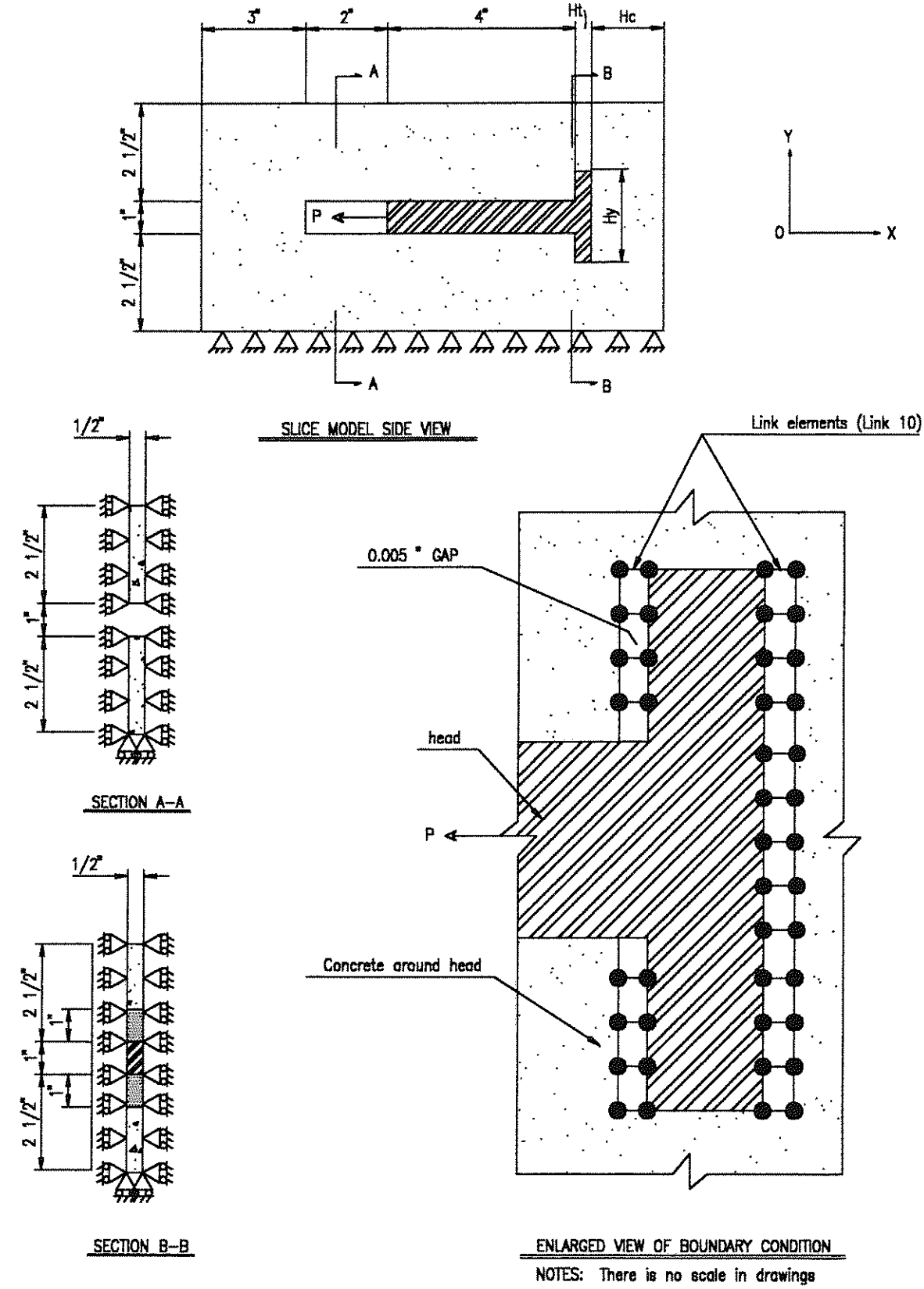
3"
2"
4"
Ht
Hc
A
B
2 1/2"
1"
2 1/2"
P
Hc
Y
O
X
A
B
SLICE MODEL SIDE VIEW
1/2"
2 1/2"
1"
2 1/2"
SECTION A-A
1/2"
2 1/2"
1"
1"
1"
2 1/2"
SECTION B-B
Link elements (Link 10)
0.005 " GAP
head
P
Concrete around head
ENLARGED VIEW OF BOUNDARY CONDITION
NOTES: There is no scale in drawings

Fig. 5.1-1

nonlinear behavior can be employed. One of these variables is the concrete tension strength, which is assumed to be 400 psi. Also, two coefficients regarding the shear capability along the faces of the cracked concrete are used. The recommended values for these factors are within the range of 0.0 to 1.0 according to ANSYS. Based on engineering judgment, two factors, "shr-cl" and "shr-op", in terms of shear transfer effectiveness, are assumed to be 0.7 and 0.2 for closed crack and open crack, respectively. This assumption means that after a crack appears in the concrete, 70 percent of nominal shear capacity is presumed if crack is in closed, while 20 percent of nominal shear capacity is assumed if crack is in open.

Only one load level used in each of these two models. The applied load is 3,530 lb. and this is equivalent to a nominal reference compressive stress of 3,530 psi over the concrete bearing face, because the "effective" contact area is 1 in^2. Also, the loads are defined as two concentrated forces applied on two nodes at the tip of the bar. The input of the major parameters for these two models is listed on the next page for reference.

Input Parameters for Slice 1 & Slice 2 Models

Item	Value	Remark
1. Finite Elements:		
concrete and steel	ANSYS solid 42	
concrete and steel	ANSYS solid 45	in Slice 1 for both concrete and steel, in Slice 2 for steel only
concrete	ANSYS solid 65 (8 node element)	in Slice 2 for concrete only
concrete and steel links	ANSYS link 10	
2. Modules of Elasticity:		
steel	$E_s = 29.0 \times 10^6$ psi	
concrete	$E_c = 3.8 \times 10^6$ psi	
3. Poisson's ratio:		
steel	$\mu_s = 0.3$	
concrete	$\mu_c = 0.2$	
4. Geometry:		
bar area	$A_b = 0.5$ in ^{2}	(A_b = 0.5 in. × 1 in.)
head thickness	$H_t = 0.5$ in	
head area	$A_t = 1.5$ in ^{2}	(A_t = 0.5 in. × 3 in.)
long edge of head	$H_y = 3.0$ in	
short edge of head	$H_z = 0.5$ in	(thickness of slice)
cover behind head	$H_c = 3$ in	
5. Load:		
P	3,530 lb.	Assumed

Notes: The value and situation are the same in both Slice 1 & Slice 2 if there is no specific entries in the remark column.

5.2 Comparisons of Results

Similar to the presentation of the results in the advanced 3D linear model, several color plots are used to show the stress distributions over the concrete slice models and to make comparisons of results of interest. Slice 1 and Slice 2 will be made through this section. The variables selected for comparison are normal compressive stresses for the concrete in the slices.

Generally, the normal compressive stresses distribution patterns over the concrete in Slice 1 and Slice 2 are similar in terms of the shape of the stress distribution field. This results is expected due to the same model size, load, and boundary condition being used in both Slice 1 and Slice 2. However, the stress level and stress concentration factor are different. Also, there are different features in some localized stress variations, indicating that Slice 2 does exhibits nonlinear behavior.

For Slice 2, the normal compressive stress distribution over the concrete is displayed in Fig. 5.2-1. The concrete slice, with stress distribution contour, pictorially removed from the whole Slice 2 model by using selection operation as used in all previous models. The plot shows that stress level varies from -5343 psi to -280 psi. The maximum value appears at the location immediately under head and decreases in both lateral and longitudinal directions with increasing distance from the interface of the head and concrete bearing face. The maximum stress concentration factor is about 1.51, based on a nominal reference compressive stress of 3530 psi.

In order to make comparison between the results from Slice 2 and Slice 1 and to have a clearer view of the stress distribution around the concrete in front of the head, two enlarged oblique plots of stress contours for Slice 2 and Slice 1 are selected. Fig. 5.2-2 and Fig. 5.2-3 display the stress (SX) variations over Slice 2 and Slice 1, respectively.

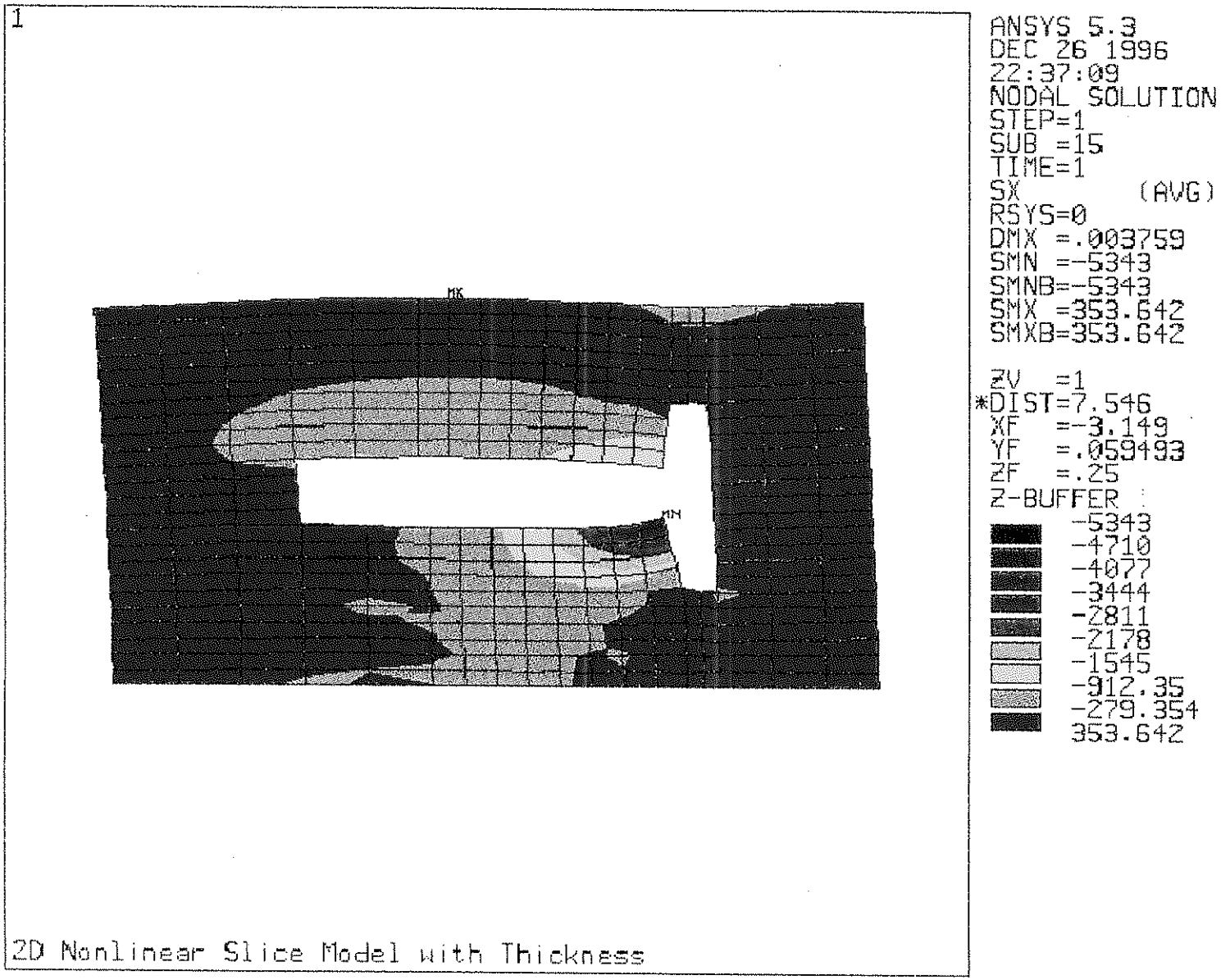
1
ANSYS 5.3
DEC 26 1996
22:37:09
NODAL SOLUTION
STEP=1
SUB =15
TIME=1
SX (AVG)
RSYS=0
DMX =.003759
SMN =-5343
SMNB=-5343
SMX =353.642
SMXB=353.642
ZV =1
*DIST=7.546
XF =-3.149
YF =.059493
ZF =.25
Z-BUFFER
-5343
-4710
-4077
-3444
-2811
-2178
-1545
-912.35
-279.354
353.642
MX
MN
2D Nonlinear Slice Model with Thickness

Fig. 5.2-1

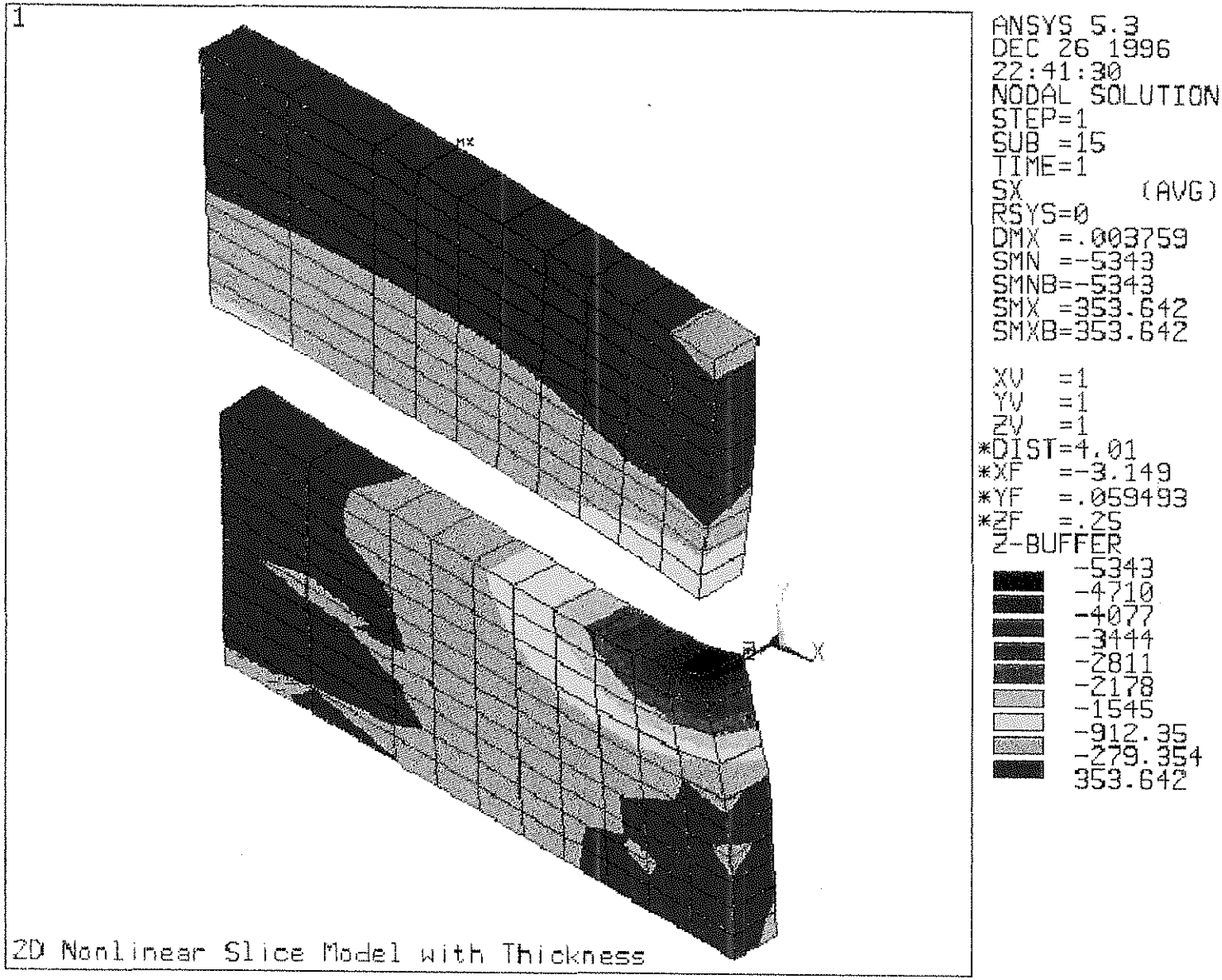
1
MX
ANSYS 5.3
DEC 26 1996
22:41:30
NODAL SOLUTION
STEP=1
SUB =15
TIME=1
SX (AVG)
RSYS=0
DMX =.003759
SMN =-5343
SMNB=-5343
SMX =353.642
SMXB=353.642
XV =1
YV =1
ZV =1
*DIST=4.01
*XF =-3.149
*YF =.059493
*ZF =.25
Z-BUFFER
-5343
-4710
-4077
-3444
-2811
-2178
-1545
-912.35
-279.354
353.642
2D Nonlinear Slice Model with Thickness

Fig. 5.2-2

1
ANSYS 5.3
DEC 26 1996
20:25:27
NODAL SOLUTION
STEP=1
SUB =1
TIME=1
SX (AVG)
RSYS=0
DMX =.004072
SMN =-8413
SMNB=-11734
SMX =928.542
SMXB=3468
-8413
-7375
-6337
-5299
-4261
-3223
-2185
-1147
-109.374
928.542
Z
X
2D Linear Slice Model with Thickness

Fig. 5.2-3

By studying Fig. 5.2-3, it can be seen that stress distribution over Slice 1 lies within the range of -8413 psi to -110 psi. The maximum stress concentration factor is about 2.26. The contour of the stress distribution field is more smooth than that of Slice 2. Based on the above information there are several differences in stress distribution behavior between the nonlinear model of Slice 2 and linear model of Slice 1.

First, the maximum stress values are different though loading condition is same. In Slice 2 the maximum stress level is about -5343 psi, while in Slice 1 the maximum stress is about - 8000 psi. Note that judgment was employed and a small number of highly stressed points were not included in this range. Even so, the comparison indicates that the nonlinear behavior of Slice 2 versus the linear behavior of Slice 1 make this large a difference. In Slice 1 the stress reaches a high level as expected because of model's linear behavior. Whereas, in Slice 2 the stress is lower compared to Slice 1 due to the model's capability of redistributing stress over the concrete slice. The "concrete" in Slice 2 can be locally crushed and cracks can develop within the concrete so that the more concrete volume is forced to share the load. This conclusion can be shown by examining the shape of stress distribution field over the lower part of the model. In Fig. 5.2-2 the field is relatively larger than that of shown in Fig. 5.3-3, which means that in Slice 2, more of the concrete volume is involved in resisting the load. The edge of stress distribution field is rougher than that of the Slice 1, and this also means that the rough shape is indication of crack development in the concrete. As a result of this nonlinear behavior in slice 2, the maximum stress is reduced, as expected.

Second, the overall stress concentration levels in both Slice 2 and Slice 1 are different. This situation can be verified by stress concentration factors and stress variation behavior in both cases. Using the stress concentration factor as a measurement, it can be seen that in Slice 2, the stress concentration factor is about 1.51, while in Slice 1 the stress concentration factor is about 2.26 or even more at some individual points. On the other hand, in both models the stress variation ranges also are different. This behavior is indicated in the color legends showing stress levels in Figs. 5.2-2 and 5.2-3. For Slice 2

the compressive stress variation is from -5343 psi to -280 psi, with an average value of about -2800 psi. Whereas, in Slice 1 the compressive stress changes from -8413 psi to -110 psi, with an average value of about - 4200 psi. Although the average stress level does not reflect the real stress distribution in a real structure, as mentioned in preliminary model investigation, but rather the stress concentration along the bearing area. However, the comparison of average stress levels for both models here does make sense for understanding that nonlinear model has a relatively lower overall stress level than that of linear model. From this point of view, it can be concluded that using the linear model results as a reference for design is generally more conservative than using the nonlinear results, but would result in more cost. Considering that the nonlinear situation does exist in real structures, using design information based on both linear and nonlinear analysis might be more reasonable and more practical than using either nonlinear or linear information alone.

In addition to the above comparisons, there also are some similarities in both of these analysis. One typical situation is that in both models, the maximum stresses are higher than the assumed concrete compressive strength of 4500 psi. In Slice 2, for example, the expected stress level should be a value around 4500 psi. Because of the nonlinear properties of the solid element 65, however, the maximum stress reaches 5343 psi. The maximum stress increased about 18.7 percent compared to the nominal concrete strength. So, there is another factor involved, that of the concrete bearing strength increase due to the triaxial stress status, and is 1.187 in this case. Also, the stress distribution field in the lower part of Slice 2 is smaller than that of the upper part of the model, but the stress is higher in the area close to the concrete bearing face. This result is due to the fact that the lower part of slice has more restraints from the supports at the bottom face and the confinement in the Z direction at both the front and back faces of the slice. In short, the more restraint, the more the reaction. A similar situation exists in Slice 1. indicating that the over-stressed situations exist in the solid structure due to the triaxial stress state within relatively highly stressed region of the concrete volume.

5.3 Summary

Since both the linear model Slice 1 and nonlinear model Slice 2 used same model size, load level, and boundary conditions, the general behavior of normal compressive stress distribution over the concrete slice are basically the same in terms of the shape of the stress distribution field within the concrete. Therefore, both linear and nonlinear models add credit to each other, which means that they provide meaningful reference information to each other to prove the accuracy of these two models. This result provides a basis for comparison between the linear and nonlinear model performance. This result also means that it is a fair substitution to compare the 3D linear and the 2D slice nonlinear models in terms of finding the differences of overall stress status and stress concentration situation.

The average stress in the nonlinear model is lower than that of the linear model. In Slice 2 the average compressive stress is about 2800 psi while in Slice 1 it is about 4200 psi. At the same time, the stress concentration level in the nonlinear model also is lower than that of the linear model, as indicated by the stress variation over concrete shown in related plots. Also, the differences in maximum stress concentration factors in both models have shown this situation. In Slice 2 the maximum stress concentration factor is about 1.51, while in Slice 1 the factor is about 2.26. Therefore, the comparison of these two models shows that the compressive stress distributes more evenly in the nonlinear case than that in linear situation, and the nonlinear behavior reflected by Slice 2 would be closer to the situation in a real structure.

Based on the above information, using linear model results, like stress concentration factor as reference for design, is more conservative than using nonlinear results. Considering cost in practice, engineering judgment is needed to make choices and design reference data that lies between linear analysis and the nonlinear condition might be considered.

CHAPTER 6

Sample Design Formula

In this chapter several preliminary design formulas for headed reinforcing bar applications will be developed based on the information obtained in this Finite Element analysis work. The formulas proposed are simplified as much as possible based on engineering judgment. The formulas and methods presented in this chapter are first steps , however, none can be applied with confidence to real applications without more advanced theoretical analysis and comparison to experimental data.

6.1 Introduction

The purpose of using a headed bar is to obtain quick anchorage for the bar in terms of full or partial replacement of the bar development length. Since there are many factors related to head's capability of doing so, the consideration of full and partial replacement of bar development length will be included in sample design formulas. For development of sample formulas, the following major factors and assumptions related to the head and concrete interactive behavior will be taken into account:

1. ***Bar size and steel strength.*** These two variables determine the maximum design force in the bar itself and to that applied to the head and associated concrete. The maximum design load is defined as the bar cross sectional area times the steel yield strength. The design of the connection between the head and the bar is not within the scope of this investigation.

2. ***Head area, thickness, and steel strength.*** These variables affect the head strength and its stiffness. As a matter of fact, they influence the stress distribution and stress concentration intensity in the concrete directly. Therefore, these are important factors in headed reinforcement applications. Simply put, it is an answer to the question of " how big a head should be used on the reinforcing bar in a given concrete strength condition".

3. ***Concrete compressive strength, stress concentration factor, and concrete strength increase factor.*** Instead of using a concrete strength reduction factor as commonly used in design practice, the concept of stress concentration is introduced in the sample formula. Using a stress concentration factor is intended to provide an emphasis on the individual characteristics of the structure. As in the case of the head applications, the head area and thickness do change the stress distribution in the concrete bearing face depending on the ratio of the head area to the bar area and the bending stiffness of the head plate. Due to the resulting triaxial stress state existing in real structures, the increase in concrete bearing capacity is considered by using factor for concrete strength increase. Experiments and companion finite element models can be used to produce tables or curves for these factors for different head sizes and concrete strengths. This also is beyond the scope of this project. However, ignoring the increase in concrete strength under triaxial stress generally is overly conservative.

4. ***Calculated effective concrete bearing area.*** It is assumed that the concrete behavior under the head compression is similar to concrete bearing under a column base plate or similar situation. In the traditional method of dealing with bearing strength problems, a direct loaded area A1 is used and another area A2 is defined so that the value of $\sqrt{A2/A1}$ (≤ 2) can be used as a factor for increasing the concrete bearing capacity. Unlike the traditional approach, in this investigation an effective concrete bearing area is defined as a ring area which is larger than the directly loaded area. This assumption is based on the information provided by the finite element models analyzed in this investigation.

5. ***Development length reduction factor and minimum development length.*** If the concrete bearing capacity, which is the result of the head and concrete interacting, is larger than the maximum design load, the head can be used as the full replacement for the bar development length. Even so a minimum nominal development length of 4 in. is recommended. The reason for doing so is that the compressive stress level is fairly high within the region from the front face of the head to about 4 in. away from the face, based on the finite element results. In other words, the concrete within this region should not be considered for use in ordinary bar development, but should be "reserved" for the use by concrete bearing stresses. Therefore, a minimum nominal development length or "an extra bar length" is needed in addition to the head usage. On the other hand, if the head is not sufficient to provide full replacement for the bar development length, determined as per the ACI Building Code, the concept of partial replacement for bar development could be introduced. That is, a development length reduction factor could be applied to bar development length, based on the ACI Building Code procedure. More explanation and two detailed examples will be presented in later sections of this chapter.

6. ***Concrete cover.*** Although the factor of concrete cover over the bar will not appear in the sample design formulas, the minimum requirement for the concrete cover is assumed to be the larger of $2\mathbf{d_b}$ and $0.707\mathbf{a}$, where $\mathbf{d_b}$ is the bar diameter, and **a** stands for the edge length of the head. This assumption is based on the consideration of providing reasonable concrete cover for the bar and bearing concrete for the head as well.

6.2 Design Formulas and Procedures

The factors and assumptions discussed in the previous section provide a basis of establishing design criteria for headed bar applications. As mentioned before, the purpose of using a headed bar is to provide quick anchorage for a reinforcing bar in situations where development is needed but the room for it is limited. In other words, in practice using a headed bar is intended to replace the partial or full bar development length depending on individual situation.

Assume that the maximum design load and concrete bearing capacity are determined by formulas (6.2-1) and (6.2-2), respectively. If the maximum design load is less than or equal to the concrete bearing capacity, the head can be used as full replacement for the bar development, otherwise partial replacement condition has to be considered. The following formulas are developed based on above assumption.

Formula (6.2-1) gives maximum design load:

$$\mathbf{P_s = A_b} f_y \qquad (6.2\text{-}1)$$

Where P_s = maximum design load

A_b = bar cross sectional area

f_y = steel yield strength

Use formula (6.2-2) to calculate concrete bearing capacity:

$$\mathbf{P_c = (K_{cm} / K_{sc})\, A_c}\, f_c' \qquad (6.2\text{-}2)$$

Formula (6.2-2a) is for calculation of effective concrete bearing area:

$$A_c = \pi/4 \, (2\, a^2 - d_b^2) \qquad (6.2\text{-}2a)$$

Where P_c = concrete bearing capacity

K_{cm} = factor for concrete strength increase 1.1 ~ 1.2

K_{sc} = factor for stress concentration (taken as 1.55 or 1.5 when the ratio of head thickness H_t to head plate cantilever length, b, is within 0.6~0.8)

A_c = calculated effective concrete bearing area (see Fig. 6.2-1 for further definition)

a = edge length of square head plate

d_b = diameter of bar

f_c' = concrete compressive strength

To examine if the head can be used for full or partial replacement of the bar development length, case A and case B give the conditions:

Case A:

$$\mathbf{P_s \le P_c} \qquad (6.2\text{-}3)$$

$$\mathbf{L_{dt} = L_{min}} \qquad (6.2\text{-}3a)$$

In Case A, the head can be used as full replacement of the bar development length, but a minimum total nominal development length of 4 in. is still recommended, as discussed in the previous section.

Case B:

$$\mathbf{P_s > P_c} \qquad (6.2\text{-}4)$$

$$\mathbf{L_{dt} = K_r \, L_d + L_{min}} \qquad (6.2\text{-}4a)$$

$$\mathbf{K_r = 1 - P_c / P_s} \qquad (6.2\text{-}4b)$$

$$\mathbf{0 < K_r < 1.0} \qquad (6.2\text{-}4c)$$

In Case B, the head can be used as partial replacement of the bar development length that is determined per the ACI Building Code.

Where L_{dt} = total bar development length required

K_r = development length reduction factor

L_d = required development length per the ACI Building Code provisions

L_{min} = 4 in.

Note: If P_c =0, then L_{min} = 0, which means no head is applied.

Practically, Case B may often appear in headed bar applications due to conditions such as limited head size in individual application, concrete strength, bar spacing and concrete cover requirements, etc. For both Cases A and B, if the stress concentration factor is employed to have more effective interactive performance of the head and concrete, as intended in formula development, it is more likely the head bending stiffness controls the design rather than the head strength. However, the head strength also should be checked by treating the head as a two-way cantilever plate, even though this is conservative. The strength design of head is basically controlled by the principal stress $\sigma 1$ as discussed in finite element models. Based on the above assumption a simplified formula for checking the head strength in terms of principal stress $\sigma 1$ is given in formula (6.2-5) See Fig. 6.2-1 for more detailed definition.

To check the head strength, formula (6.2-5) is recommended:

$$(1.5\, P_t / g)\, [\, 1 + (\, 1 + 0.44\, g\,)^{1/2}\,] \leq f_y \qquad (6.2\text{-}5)$$

Where $P_t = P_s / A_{te}$ (nominal net pressure under the head effective area)

$A_{te} = A_t - A_b$

A_t = head area

A_b = bar cross sectional area

$g = (H_t / b)^2$

H_t = head thickness

$b = (a - d_b) / 2$

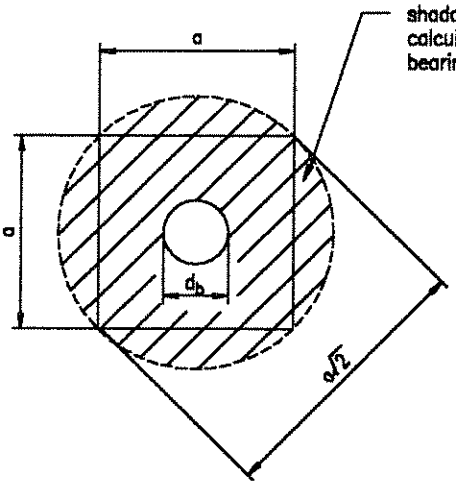

Fig. 6.2–1a

Formula (6.2–2a) is defined as:

$$Ac = \frac{(a\sqrt{2})^2}{4}\pi - Ab$$

$$= \frac{a^2}{2}\pi - \frac{d_b^2}{4}\pi$$

$$= 0.25\pi\,(2a^2 - d_b^2) \qquad (6.2\text{–}2a)$$

Where

Ab = re–bar cross section area
d_b = diameter of bar
a = edge length of head area

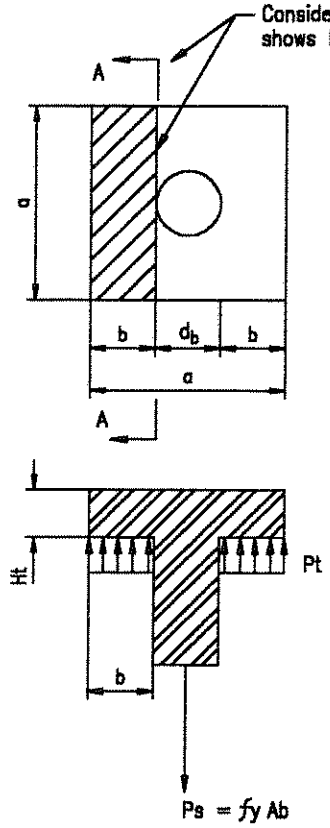

Fig. 6.2–1b

Treat the T–head as two–way cantilever plate , the principal stress S1 resulted from Pt at section A–A is developed as:

Assume $Pt = Ps / Ate$
$Ate = At - Ab$

Then, $M = (1/2)(aPt)\,(b^2) = (1/2)ab^2 Pt$

Stress due to bending:

$$\sigma = \frac{M}{I}\frac{Ht}{2} = \frac{6M}{aHt^2} \qquad (a)$$

$$= 3(b/Ht)^2 Pt$$

Stress due to shear:

$$\tau = (abPt)(aHt) = (b/Ht)Pt \qquad (b)$$

Therefore, the principal stress σ_1 :

$$\sigma_1 = (1/2)\sigma + (1/2)\sqrt{\sigma^2 + 4\tau^2} \qquad (c)$$

Replace σ and τ in (c) with (a) and (b) and simplify:

$$\sigma_1 = \frac{3b^2 Pt}{2Ht^2}\,[\,1 + \sqrt{1 + (4/9)\,(Ht/b)^2}\,] \qquad (d)$$

Let $g = (Ht/b)^2$ and put it into above formula (d), then, it yields the formula (6.2–5):

$$\sigma_1 = \frac{1.5Pt}{g}\,[\,1 + \sqrt{1 + 0.44g}\,] \leq fy \qquad (6.2\text{–}5)$$

Where

Ht = T–head thickness
$b = (a - d_b)/2$
At = T–head area

Fig. 6.2-1

6.3 Design Examples

Example 6.3-1

In a headed bar application, examine the head and bar behavior and determine the required total bar development length under the conditions given below:

8 bar, d_b = 1 in., f_y = 60,000 psi; concrete strength f_c' = 4,000 psi; head size = 2.8 in. x 2.8 in.;

Assuming $H_t/b = 0.6$; $K_{cm} = 1.2$, $K_{sc} = 1.55$.

Solution:

1) Determine maximum design load corresponding to yield of the bar

use formula (6.2-1)

$P_s = A_b f_y$

$= (0.5^2) \pi (60{,}000)$

$= 47{,}124$ lb.

2) Determine concrete bearing capacity

from formula (6.2-2a)

$A_c = 0.25 \pi (2a^2 - d_b^2)$

$= 0.25 \pi (2 \times 2.8^2 - 1^2)$

$= 11.53$ in^2

from formula (6.2-2)

$P_c = (K_{cm} / K_{sc}) / A_c f_c'$

$= (1.2 / 1.55) / (11.53) (4{,}000)$

$= 35705$ lb.

$P_s > P_c$ Case B applies

3) Determine total required development length after the head is employed.

Assume $L_d = 30$ in. is required per the ACI Building Code if no head is used.

From (6.2-4a)

$L_{dt} = K_r L_d + L_{min}$

$= (1 - P_e / P_s) L_d + L_{min}$

$= (1 - 35705 / 47124) (30) + 4$

$= 11.3$ in.

4) Check head strength

Use formula (6.2-5)

$Ate = At - Ab$

$= 2.8^2 - 0.5^2 \pi$

$= 7.055$ in^2

$P_t = P_s / A_{te} = 47124 / 7.055 = 6680$ psi

$\sigma 1 = (1.5 P_t / g) [1 + (1 + 0.44 g)^{1/2}]$

$= (1.5 \times 6680 / 0.6^2) [1 + (1 + 0.44 \times 0.6^2)^{1/2}]$

$= 57{,}790$ psi $< f_y = 60{,}000$ psi OK

Known: $H_t / b = 0.6$

$H_t = 0.6\ b$

$= 0.6 (a - d_b) /2$

$= 0.6 (2.8 - 1) /2 = 0.54$ in.

Thus, using 2.8 x 2.8 x 0.54 head on a reinforcing bar with 11.3 in. development length corresponds to a L_d of 30 in. This result does not include any effect of confinement on the reduction in development length, and the headed bar relies only on the head for anchorage. Also, effects of cover are ignored.

Example 6.3-2

Determine the head size for full replacement of bar development length based on conditions below:

6 bar, $d_b = 0.75$ in., $f_y = 60{,}000$ psi;

concrete strength $f_c' = 4{,}000$ psi;

assuming $H_t / b = 0.8$, $K_{cm} = 1.2$, $K_{sc} = 1.5$

Solution:

1) Determine maximum design load

$$P_s = A_b f_y$$

$$= (0.44) (60{,}000) = 26{,}400 \text{ lb.}$$

2) Determine head size

Let $P_c = P_s = 26{,}400$ lb.

from formula (6.2-2)

$$A_c = P_c K_{sc} / K_{cm} f_c'$$

$$= (24{,}600) (1.5) / (1.2) (4{,}000)$$

$$= 7.69 \text{ in}^2$$

from formula (6.2-2a)

know:

$$a = [(A_c / 0.25 \pi + d_b^2) / 2]^{1/2}$$

$$= [(7.69 / 0.25 \pi + 0.75^2) /2]^{1/2}$$

$$= 2.28 \text{ in.}$$

$$b = (a - d_b) /2 = (2.28 - 0.75) / 2 = 0.765 \text{ in.}$$

$$H_t = 0.8\ b = (\ 0.8\ )\ (\ 0.765\ ) = 0.61\ \text{in.}$$

3) Minimum bar development length applies.

$P_s = P_c$ Case A

$K_r = 0$ $L_{dt} = 0 + L_{min} = 4$ in.

4) Check head strength

$A_{te} = A_t - A_b$

$= 2.28^{\ 2} - 0.44 = 4.\ 758\ \text{in}^{\ 2}$

$P_t = P_s / A_t = 26{,}400 / 4.758 = 5{,}550$ psi

$\sigma 1 = (\ 1.5\ Pt / \rho\ )\ [\ 1 + (\ 1 + 0.44\ \rho\ )^{1/2}\ ]$

$= (\ 1.5 \times 5{,}550 / 0.8^2\ )\ [\ 1 + (\ 1 + 0.44 \times 0.8^2\ )^{1/2}\ ]$

$= 27{,}734$ psi $< f_y = 60{,}000$ psi OK

Thus, using a 2.28 x 2.28 x 0.61 head on a #6 bar could be considered as full replacement as required development for # 6 bar under same condition. Providing the first 4 inches of the bar is "reserved" for bearing of the head. These results show how a headed bar might be designed for use in a typical concrete application. A key question that needs to be studied in future research in how the presence of stirrups in the "bearing region" will decrease the need for development length.

CHAPTER 7

Conclusions

This investigation of the anchorage behavior of headed reinforcing bar was studied by using the finite element method and specifically the program, ANSYS. The study has yielded useful information about headed bar and bearing concrete interactive behavior. The information from this investigation has presented the information fundamental to the understanding of head and concrete structural behavior in terms of stress distribution and stress concentration state in the head and within the concrete volume under the head. At the same time, several proposed sample design formulas for headed bar applications have been developed based on results from the Finite Element models used in this project and engineering judgment. The project has fairly provided informative "testimony" to endorse the development of headed reinforcement in certain reinforced concrete structural applications and has offered reference data for further research on headed bar applications.

As a summary or conclusion to this investigation, several points are restated below:

1. Basically, the head on the bar behaves as a two-way plate in bending and the concrete under the head is in compression, similar to concrete under well known bearing conditions. Conceptually, this assumption helps one to understand head and concrete interactive behavior and to simplify the development of future design formulas.

2. The effective anchorage property of the head in terms of providing anchorage action for the reinforcing bar has been observed through Finite Element models. The

tension force from the bar can be rapidly transferred to bearing in the concrete through the head. This transformation can be interpreted through examination of stress distribution and strain variation around the head and in concrete that is bearing under the head. The stress and strain level is high within the concrete that lies immediately under the head compression but drops quickly with distance away from the head in both the lateral and longitudinal directions. This behavior means that the anchorage action develops quickly in the concrete that is directly under head and is placed in compression; the influence of stress and strain to the rest of concrete is minor. So a typical anchor-like behavior is noted. The head can provide quick anchorage action for the bar to replace the bar development length.

3. Using a headed bar in certain reinforced concrete application not only saves steel, but also provides a good solution to "reinforcement congestion" in construction. The steel volume used for a head, that replaces an equivalent bar development length, is less than that for the bar development length per the ACI requirements. In other words, if same steel volume is used for the head and the bar development length, the head has better anchorage performance. Also, if the head is properly used, it requires less room for placement of the head in the member than that required for placement of the bar development length.

4. There are many factors related to the anchorage capacity of headed bars. The key factors are bar size, head size, concrete and steel strengths, and confinement around the concrete in the bearing zone. Bar size and its material strength determines maximum design load for the head-concrete interaction. The head size and its material strength are important because they determine head strength and stiffness that directly affect the stress distribution over concrete bearing area. Concrete strength, obviously, is a key factor in concrete bearing capacity. Since stress and strain distribution over the concrete bearing area cannot be uniform in real structures, a stress concentration factor should be considered. Due to the triaxial stress status that exists in 3D structures, a concrete strength increase is expected and a factor reflecting some degree of concrete strength

increment also should be used. More reliable values for these factors mentioned above could be obtained by conducting extensive experiment, and related advanced Finite Element analysis.

5. The design formula for checking the head strength is conservative because the head is treated as a cantilever plate and the influence of concrete behind the head is ignored. Actually, the concrete behind the head does contribute to the anchorage capacity of the head-concrete interaction, in terms of providing additional support for the head against backward deformation. So the concrete behind the head should help increase head stiffness and reduce the bending stress in the head and related stress concentration levels over concrete bearing area.

6. Based on the information from this investigation and other information from experimental work, it is recommended that in headed bar application, reinforcement be provided in front of the head to enhance the concrete confinement. It also is suggested that the use of relatively thick head to strengthen head bending stiffness. This is not only good for head itself but also reduce the stress concentration over bearing concrete so that a better head-concrete interactive situation can be achieved.

In short, through this Finite Element analysis project the information fundamental to the understanding of head and concrete structural behavior was obtained. The head behaves as a two-way plate in bending and the concrete under the head is in compression, similar to well known bearing conditions. The head can provide quick anchorage action for the bar and can be used to replace the bar development length partially or fully depending on individual applications. Based on the information from this project, sample design formulas were developed, and recommendations regarding headed reinforcing bar applications have been provided in order to offer useful information for further research on headed reinforcement.

Reference

1. R. D. Cook, D. S. Malkus, M. E. Plesha, Concepts and Applications of Finite Element Analysis, Third Edition, John Wiley & Sons, 1989.

2. C. K. Wang, C. G. Salmon, Reinforced Concrete Design, Fifth Edition, HarperCollins Inc., 1992.

3. A. H. Nilson, G. Winter, Design of Concrete Structures, Eleventh Edition, McGraw-Hill, Inc., 1991.

4. ACI Committee 318, Building Code Requirements for Reinforced Concrete (ACI 318-95) and Commentary- ACI 318R-95, Detroit, MI

5. R. L. Brockenbrough, F. S. Merritt, Structural Steel Designer's Handbook, Second Edition, McGraw-Hill, Inc., 1994.

6. W. C. Young, Roark's Formulas for Stress & Strain , Sixth Edition, McGraw-Hill, Inc., 1989.

7. Swanson Analysis Systems, Inc. Introduction to ANSYS for Revision 5.1 Vol. I Notes and Exercises , 1994.

8. Swanson Analysis Systems, Inc. Introduction to ANSYS for Revision 5.1 Vol. II Solutions to Exercises, 1994.

9. J. Wright and S. L. McCabe, "Bond and Development of Headed Reinforcing Bars", Center for Research SM Report No.44, University of Kansas, Lawrence, KS, September, 1997.

10. American Society for Testing and Materials, "Standard Requirements for Welded Headed Reinforcing Bar", ASTM A970-97, Philadelphia, 1997.